RNAi suppression of DNA methylation affects the drought stress response and genome integrity in transgenic poplar

Mamadou-Dia Sow, Anne-laure Le Gac, Régis Fichot, Sophie Lanciano, Alain Delaunay, Isabelle Le Jan, Marie-claude Lesage-Descauses, Sylvie Citerne, Jose Caius, Véronique Brunaud, et al.

RNAi suppression of DNA methylation affects the drought stress response and genome integrity in transgenic poplar

Mamadou D. Sow [1*], Anne-Laure Le Gac [1*], Régis Fichot [1], Sophie Lanciano [2,3], Alain Delaunay [1,5] Isabelle Le Jan [1], Marie-Claude Lesage-Descauses [4], Sylvie Citerne [5], Jose Caius [6], Véronique Brunaud [6], Ludivine Soubigou-Taconnat [6], Hervé Cochard [7], Vincent Segura [4,8], Cristian Chaparro [9], Christoph Grunau [9], Christian Daviaud [10], Jörg Tost [10], Franck Brignolas [1], Steven H. Strauss [11], Marie Mirouze [2,3 8] and Stéphane Maury [1 9 10]

1- LBLGC, INRAE, Université d'Orléans, EA 1207 USC 1328, 45067 Orléans, France;
2- IRD, UMR 11 232 DIADE, Université de Montpellier, 34090 Montpellier, France;
3- Université de Perpignan, 12 Laboratory of Plant Genome and Development, 66860 Perpignan, France;
4- BioForA, INRAE, ONF, 13 UMR 0588, 45075 Orléans, France;
5- Institut Jean-Pierre Bourgin, INRAE, AgroParisTech, Université 14 Paris-Saclay, 78000, Versailles, France;
6- Université Paris-Saclay, CNRS, INRAE, Université Evry, 15 Institute of Plant Sciences Paris-Saclay (IPS2), 91405, Orsay, France;
7- Université Clermont 16 Auvergne, INRAE, PIAF, 63000 Clermont-Ferrand, France;
8- UMR AGAP Institut, Université 17 Montpellier, CIRAD, INRAE, Institut Montpellier SupAgro, UMR 1334, F-34398 Montpellier, 18 France;
9- IHPE, Université de Perpignan, UMR 5244, 66100, Perpignan, France;
10- Laboratory for 19 Epigenetics and Environment Centre National de Recherche en Génomique Humaine, CEA- Institut 20 de Biologie Francois Jacob, Université Paris-Saclay, 91057 Evry, France;
11- Department of Forest 21 Ecosystems and Society, Oregon State University, Corvallis, OR 97331-5752, USA

ABSTRACT

Trees are long-lived organisms that continuously adapt to their environments, a process in which epigenetic mechanisms are likely to play a key role. Via downregulation of the chromatin remodeler DECREASED IN DNA METHYLATION 1 (DDM1) in poplar (*Populus tremula* x *Populus alba*) RNAi lines, we examined how DNA methylation coordinates genomic and physiological responses to moderate water deficit.

We compared the growth and drought response of two RNAi-*ddm1* lines to wild-type (WT) trees under well-watered and water deficit/rewatering conditions, and analyzed their methylomes, transcriptomes, mobilomes and phytohormone contents in the shoot apical meristem.

The RNAi-*ddm1* lines were more tolerant to drought-induced cavitation but did not differ in height or stem diameter growth. About 5000 differentially methylated regions were consistently detected in both RNAi-*ddm1* lines, colocalizing with 910 genes and 89 active transposable elements. Under water deficit conditions, 136 differentially expressed genes were found, including many involved in phytohormone pathways; changes in phytohormone concentrations were also detected. Finally, the combination of hypomethylation and drought led to the mobility of two transposable elements

Our findings suggest major roles for DNA methylation in regulation of genes involved in hormone-related stress responses, and the maintenance of genome integrity through repression of transposable elements.

KEYWORDS

ddm1 , DNA methylation, drought, epigenetics, hormone, mobilome, poplar, shoot apical meristem

INTRODUCTION

As long-living organisms, trees are subjected to repeated environmental challenges over their lifetimes. During recent decades, forest decline has been reported around the world due to heat and drought episodes (Allen *et al.*, 2010; Anderegg *et al.*, 2016). Survival and adaptation of populations will depend on the ability of trees to cope with rapidly changing conditions. Among the potential sources of flexibility in perennials like trees, epigenetics has received growing attention (Yakovlev *et al.*, 2012, 2016; Br€autigam *et al.*, 2013; Plomion *et al.*, 2016; Carneros *et al.*, 2017; Sow *et al.*, 2018a; Amaral *et al.*, 2020). Epigenetics is defined as the study of heritable changes that affect gene expression without changing the DNA sequence (Russo *et al.*, 1996). Considerable efforts have been made to unravel the role of epigenetics in plant developmental processes, stress responses and adaptation, but primarily in annuals (Slotkin & Martienssen, 2007; Colome-Tatche *et al.*, 2012; Cortijo *et al.*, 2014; Kooke *et al.*, 2015; Raju *et al.*, 2018; Schmid *et al.*, 2018), while its role in perennials like trees still needs clarification (Amaral *et al.*, 2020).

DNA methylation is one of the most studied epigenetic marks (Zhang *et al.*, 2018a). It is important in both plants and mammals for many biological processes, such as imprinting, and its disruption can lead to developmental abnormalities (Vongs *et al.*, 1993; Zemach *et al.*, 2013; Zhang *et al.*, 2018b). In addition to controlling gene expression, DNA methylation is also involved in the maintenance of genome integrity by silencing transposable elements (TEs), preventing them from spreading within the host genome (Fultz *et al.*, 2015; Ikeda & Nishimura, 2015). DNA methylation is required to silence TEs located in the heterochromatin, and a decrease in DNA methylation level can result in their reactivation (Lippman *et al.*, 2004; Mirouze *et al.*, 2009; Mirouze & Paszkowski, 2011). One of the bestknown examples of the control of TEs by DNA methylation comes from the study of mutants of chromatin remodeling complexes which are involved in maintenance of DNA methylation, such as *Decreased DNA Methylation I* (*DDM1*, a SWI/SNF family member). Its depletion affects the distribution of methylation in all sequence contexts (Vongs *et al.*, 1993; Zemach *et al.*, 2013; Zhu *et al.*, 2013). *DDM1* was first identified in Arabidopsis through a forward genetic mutant screen causing a 'decrease in DNA methylation' (Vongs *et al.*, 1993). Several studies further characterized *ddm1* mutants in Arabidopsis (Saze & Kakutani, 2007; Yao *et al.*, 2012; Zemach *et al.*, 2013; Cortijo *et al.*, 2014; Ito *et al.*, 2015; Kawanabe *et al.*, 2016), turnip (Fujimoto *et al.*, 2008; Sasaki *et al.*, 2012), maize (Li *et al.*, 2014), and rice (Higo *et al.*, 2012; Tan *et al.*, 2016). Recently *DDM1* has been shown to mediate the deposition of H2AW, a histone variant important for heterochromatin (Osakabe *et al.*, 2021) ;

In poplar trees, RNAi-*ddm1* lines have been previously obtained by targeting the transcripts of the two orthologous *DDM1* paralogs in *Populus tremula* x *Populus alba* cv INRA 717-1B4 (Zhu *et al.*, 2013). Under standard glasshouse conditions, the regenerated lines did not show developmental defects, although newly formed leaves displayed necrotic spots after a cycle of dormancy (Zhu *et al.*, 2013). These lines, which have been stabilized *in vitro* for several years now, represent valuable tools with which to clarify the functional role of DNA methylation in perennials such as forest trees. As a model tree with important genomic resources (Tuskan *et al.*, 2006; Jansson & Douglas, 2007), poplar (*Populus* spp.) has been a prime system for the study of the ecophysiological and molecular bases of the drought response (Monclus *et al.*, 2006; Street *et al.*, 2006; Bogeat-Triboulot *et al.*, 2007; Cohen *et al.*, 2010; Hamanishi *et al.*, 2012; Fichot *et al.*, 2015). Differences in global DNA methylation levels among poplar hybrid genotypes have been shown to correlate with biomass production under water deficit (Gourcilleau *et al.*, 2010; Raj *et al.*, 2011; Le Gac *et al.*, 2019). Epigenomic analyses have further shown that water deficit induces targeted changes in DNA methylation patterns at phytohormone-related genes, thereby favoring phenotypic plasticity (Lafon-Placette *et al.*, 2018). This has raised the question of a possible link between epigenetics and phytohormone signaling/ synthesis in the regulation of plant plasticity, particularly in primary meristems where development is initiated (Maury *et al.*, 2019). In addition, it has been shown that winter-dormant shoot apical meristems (SAMs) of poplars grown under field conditions can keep an epigenetic memory of a summer drought experienced during the growing season through modifications in DNA methylation (Le Gac *et al.*, 2018; Sow *et al.*, 2018b). The role of epigenetic memory in trees, besides poplar, in response to biotic and abiotic stresses or priming is becoming increasingly documented (Yakovlev *et al.*, 2014; Carneros *et al.*, 2017; Gömöry *et al.*, 2017; Yakovlev & Fossdal, 2017; Amaral *et al.*, 2020) ;

So far, most of the studies conducted in trees focusing on DNA methylation and gene expression have used a correlative approach. For example, extensive gene-body methylation is found in open

chromatin, is linked to structural gene characteristics, and correlates with tissue-specific gene expression or stress (Vining *et al.*, 2012; Bräutigam *et al.*, 2013; Lafon-Placette *et al.*, 2013, 2018; Liang *et al.*, 2014). Here, we employed a reverse genetic approach using RNAi-*ddm1* poplar lines to investigate the functional impact of variations in DNA methylation under water deficit conditions. We combined a fine-scale ecophysiological characterization of water deficit responses and growth dynamics with hormone profiling and integrative (epi)genomics in the shoot apical meristem of the hypomethylated RNAi-*ddm1* lines.

MATERIAL AND METHODS

Plant material, experimental design and control of water deficit

Experiments were conducted on two *PtDDM1* RNAi lines (*ddm1* -15 and *ddm1* -23) and a wild type (WT) line of *Populus tremula* x *Populus alba* (clone INRA 717-1B4). These two RNAi-*ddm1* lines were chosen among those previously described by Zhu *et al.* (2013) as they consistently displayed lower levels of Pt*DDM1* residual expression (38.0% and 37.5% for *ddm1* -15 and *ddm1* -23, respectively) and a decrease of cytosine methylation levels (decrease of 17.0 and 16.7%, respectively) compared to WT. These characteristics were confirmed in the present study. The experiment was conducted in a controlled glasshouse on 4-l potted saplings (see Supporting Information Methods S1 for detailed growth conditions). In total, 81 plants were randomly distributed into nine blocks and assigned to either a well-watered control treatment (WW, one individual of each line per block) or a water deficit treatment followed by rewatering (WD-RW, two individuals of each line per block) (Fig. 1).

Water deficit was initiated at t_0 on 3-month-old plants and lasted for 3 wk until t_1. Plants from the WW condition were kept watered at close to field capacity, while plants from the WD-RW condition were watered to a target value of 40% of relative extractable water (REW, see Methods S1 for detailed information on the control of water deficit). At t_1, three blocks were destructively harvested while the six blocks remaining were rewatered and maintained at field capacity before being sampled 1 wk later (t_2). As the focus of this study was on post-stress epigenomic events, the blocks sampled at t_1 were not considered in this study and the measurements reported hereafter were systematically performed on the six remaining blocks (n = 6 for WW, n = 12 for WD-RW) except where another subset is specified.

The intensity of water deficit was evaluated at t_1 by measuring predawn leaf water potential (Ψ_{pd}, MPa) before rewatering.

Measurements were performed on a subset of five randomly selected blocks using a pressure chamber (PMS instruments, Albany, OR, USA; n = 5 for WW, n = 5 for WD-RW). Minimum leaf water potential (Ψ_{min}) was estimated for the same plants at midday on the day preceding rewatering.

Physiological and phenotypic characterization

Assessment of growth and leaf phenotypes

Stem height was measured every 2 d using a telescopic ruler, while stem diameter was measured every 4 d using a digital caliper. We also repeatedly measured the number of leaves showing necrotic spots (mottled leaves, see Zhu *et al.*, 2013) during the whole duration of the experiment and counted the number of leaves showing a 'folded' morphology. These measurements were performed on all plants (n = 6 for WW, n = 12 for WD-RW).

Leaf traits

Leaf gas exchange was assessed every day during the experiment (n = 5 per line for WW and WD-RW). Bulk leaf carbon isotope composition (∂13C) was measured at t_2 from a mature leaf on all plants (n = 6 for WW, n = 12 for WD-RW) while stomatal density was assessed on a subset of three blocks (n = 3 for WW and WD-RW). See Methods S1 for detailed procedures for stomatal conductance, carbon isotope composition and stomatal counts.

Xylem vulnerability to drought-induced cavitation

Xylem vulnerability to drought-induced cavitation was assessed at t_2 on stems of all plants under the well-watered condition only (n = 6) (INRAE Phenobois Platform, Clermont-Ferrand, France). We used the Cavitron technique, which is well suited to poplars (Cochard *et al.*, 2005; Fichot *et al.*, 2015). The xylem tension causing a 50% loss of hydraulic conductance (P50, MPa) was used to compare vulnerability. See Methods S1.

Phytohormone quantification

Phytohormone assays for abscisic acid (ABA), free auxin, salicylic acid (SA), jasmonic acid (JA) and cytokinins were performed on the individual SAMs collected at t_1 (n = 3 for each line and condition) using liquid chromatography–mass spectrometry (LC-MS) according to a previously published procedure (OVCM platform, IJPB, INRAE Versailles, France; Li-Marchetti *et al.*, 2015; Trapet *et al.*, 2016). For more details, see Methods S1.

DNA extraction and determination of global DNA methylation levels by high-performance liquid chromatography (HPLC)

Genomic DNA was extracted from individual SAMs (n = 3 for each line for each water condition at t_2) using a cetyl trimethylammonium bromide (CTAB) protocol (Doyle & Doyle, 1987), and was stored at -80°C. Quantity and quality were approximated using a NanoDrop spectrometer (Thermo Fisher Scientific, Waltham, MA, USA). For the HPLC determination of global DNA methylation, we followed the method described by Zhu *et al.* (2013).

Methylome analyses using whole genome bisulfite sequencing (WGBS)

An equimolar pool of 2 µg DNA at *c*. 100 ng μl^{-1} was made for each line in each treatment from four individual SAMs (n = 4; at t_2). Whole-genome bisulfite sequencing was performed at the Centre National de Genotypage (CNRGH; Evry, France) in accordance with the procedure described by Daviaud *et al.* (2018), adapted from the library preparation kit manufacturer's online instructions (http://www.nugen.com/products/ovationultralow-methyl-seq-library-systems) (see Methods S1). The sequencing was performed in paired-end mode (2 x 150bp) on an Illumina HiSeq4000 platform. Raw data were stored as FASTQ files with a minimal theoretical coverage of 30x.

The bioinformatic pipeline for methylome analysis was adapted from the ENCODE pipeline (https://www.encodeprojec t.org/data-standards/wgbs) and installed on the Galaxy instance of the Interactions H^otes Pathogenes Environnements (IHPE) platform (http://galaxy.univ-perp.fr/, Perpignan, France) using the reference genome *Populus tremula* x *Populus alba* (http:// aspendb.uga.edu/index.php/databases/spta-717-genome). For more details, see Methods S1.

Transcriptomic analyses

We performed RNAseq on samples obtained in WD-RW conditions to compare one RNAi-*ddm1* line (*ddm1-23*) to the WT. The line *ddm1-23* was chosen as the most representative of the two lines as it showed a smaller decrease in methylation compared to *ddm1-15*, and most of its DMRs were common to *ddm1-15* (see the Results section). Total RNA was extracted from SAMs from three biological replicates per line (n = 3; at t_2) using a modified version of the protocol described by Chang *et al.* (1993). For more details, see Methods S1.

Mobilome-seq and copy number variation of transposable elements

We sequenced extrachromosomal circular DNAs (eccDNAs) in order to identify active TEs, as described by Lanciano *et al.* (2017). We used *c*. 6 µg of genomic DNA (the same pools used for WGBS) obtained for each line in each condition from individual SAMs (n = 4; at t_2) to prepare mobilome-seq libraries. eccDNAs were isolated and amplified and libraries were prepared and sequenced following Lanciano *et al.* (2017). Bioinformatic analyses were carried out on the *Populus tremula* x *Populus alba* genome (SPta717 v1.1) using the pipelines described by Lanciano *et al.* (2017). DNA copy number

variation of TEs was assessed for all studied lines in both conditions by quantitative polymerase chain reaction (qPCR) in triplicate. For more details, see Methods S1.

Statistical analyses

Statistical analyses were performed using the R statistical software under the R STUDIO integrated development environment (R Development Core Team, 2015; http://www.rstudio.com/). Means are represented with their standard errors (SE). When measurements were available for more than one individual replicate per block under the WD-RW condition, pseudoreplicates were averaged to yield a single value per block. Differences between lines and conditions for phenotypic traits were evaluated by analysis of variance (ANOVA) on individual values adjusted for block effects. Tukey's post-hoc test was used to identify differences between groups when ANOVAs indicated significant effects. Statistical tests were performed and *P*-values were calculated according to the methods described by Wasserstein & Lazar (2016).

RESULTS

Phenotypic and physiological differences among lines under well-watered conditions

We performed a drought experiment on WT and RNAi-*ddm1* poplar lines (Fig. 1). Plants in the control condition remained watered close to field capacity during the whole experiment. Relative extractable water (REW) never dropped below 70% (Fig. 2a) and predawn leaf water potential (Ψ_{pd}) values remained above -0.5 MPa (Fig. 2b). There was no significant difference in either REW or Ψ_{pd} among lines (Fig. 2a,b). The WT and RNAi-*ddm1* lines all showed linear growth during the experiment (Fig. S1a) and there was no significant difference for height growth rates (1.27 ± 0.03 cm d^{-1}, $P = 0.797$) or diameter growth rates (0.09 ± 0.02 mm d^{-1}, $P = 0.091$) (Fig. 3a,b). Differences among lines were, however, visible for total leaf area, with RNAi-*ddm1* lines exhibiting, on average, 28% lower values compared to the WT ($P = 0.021$, Fig. S2a), which was mainly explained by the smaller leaves in the middle canopy (Fig. S2b).

Significant differences were observed for xylem vulnerability to cavitation ($P < 0.001$, Fig. 3c). The WT was *c*. 10% more vulnerable (P_{50} =2.16 $\pm$ 0.05 MPa) compared to the RNA-*ddm1* mean; *ddm1-23* was the most resistant (P_{50} =2.45 $\pm$ 0.04 MPa), and *ddm1-15* was intermediate (P_{50} =2.28 $\pm$ 0.04 MPa). By contrast, there were no significant differences between lines for leaf traits (Fig. S3) and xylem structural or biochemical traits (Table S1).

The proportion of leaves showing necrotic spots reached 40% at the end of the experiment for *ddm1-23* and > 60% for *ddm-15*, while it remained close to zero for the WT (Fig. 4). Symptom occurrence was not linear but tended to increase at a specific physiological stage (Fig. 4), mainly on mature leaves and not in the uppermost third of the plant. The RNAi-*ddm1* lines (mostly *ddm1-23*) also exhibited leaves that tended to fold around the midvein (Fig. 4).

In summary, under well-watered conditions, RNAi-*ddm1* lines showed growth and leaf physiology similar to WT. However, RNAi-*ddm1* lines displayed necrotic spots on mature leaves and higher xylem resistance to cavitation (Table 1).

Differences in drought response

Soil water content of drought stressed plants started to exhibit significantly lower values than the control 4 d after the initiation of the water deficit. Values of REW then fluctuated between 20 and 40% until t_1 (Fig. 2a); rewatering at t1 increased REW back to control values (Fig. 2a). Predawn leaf water potential at t1 was significantly lower than in well-watered plants ($P < 0.001$ for each line) and reached *c*. -0.8 MPa with no significant difference among lines (Fig. 2b). Height and diameter growth rates during

the 3-wk water deficit were significantly reduced, by 25% and 39%, in the WT trees (Fig. 3, $P = 0.037$ and P = 0.026). By contrast, height and diameter growth rates of RNAi-*ddm1* lines were not significantly affected by water deficit (8% and 13% reduction in height growth rates with $P = 0.204$ and $P = 0.244$ for RNAi*ddm1-15* and RNAi-*ddm1-23*, respectively; 4% and 8% reduction in diameter growth rates with $P = 0.828$ and $P = 0.516$ for *ddm1-15* and *ddm1-23*, respectively). Rewatering brought growth back to the levels of the controls (Fig. S1).

In response to water deficit, stomatal conductance started to decrease *c*. 10 d after drought initiation, that is, once REW had dropped below 40% (Figs 2a, S3). The WT and RNAi-*ddm1* lines showed relatively comparable dynamics and reached almost an 80% decrease relative to controls (Fig. S3). Net CO_2 assimilation rates were less impacted, in agreement with the moderate intensity of the water deficit (Fig. S3). The WT and RNAi-*ddm1* lines all showed leaf traits that were comparable to those of the plants under the well-watered condition, although the WT did show a significant effect of water deficit for leaf $\partial^{13}C$ and stomatal density (Fig. S3). Xylem traits were seldom affected by water deficit and were not statistically different among the WT and RNAi-*ddm1* lines (Table S1). Water deficit also had no significant effect on the occurrence of leaf symptoms (Fig. 4).

In summary, RNAi-*ddm1* lines exhibited a drought response that was mostly similar to the WT in terms of leaf physiology and xylem structure/biochemical composition. However, height and diameter growth were not significantly decreased by the moderate water deficit, in contrast to the WT, suggesting enhanced stress tolerance (Table 1).

Phytohormone concentrations in shoot apices

There were no significant differences among lines in phytohormone concentrations under well-watered conditions. Salicylic acid content, however, was on average almost 2.5 times higher in RNAi-*ddm1* lines (Fig. 5). Under water deficit-rewatering conditions, significant differences among lines were observed for SA (Fig. 5); SA was still almost two times higher in RNAi-*ddm1* lines, while zeatine riboside and zeatine-O-glucoside riboside levels were on average one third lower in RNAi-*ddm1* lines (Fig. 5). Although the ABA concentrations were on average 20% lower for the RNAi-*ddm1* lines compared to WT, the results did not reach statistical significance ($P = 0.267$). Free auxin concentrations were similar among all lines (Fig. 5). The WT exhibited the lowest values among all lines for SA, and the SA concentration did not change significantly as a function of the stress conditions (Fig. 5). Concentrations of zeatine riboside and zeatine-O-glucoside riboside were higher in the WT because of a treatment-induced increase (Fig. 5). Concentrations of isopentenyladenosine showed a more complex pattern, with RNAi*ddm1-15* and RNAi-*ddm1-23* exhibiting the lowest and the highest values, respectively (Fig. 5).

In summary, RNAi-*ddm1* lines differed from the WT, mostly under water deficit for SA (higher) and cytokinin (lower) concentrations (Table 1; Fig. 5) suggesting a physiological change in the hormonal balance ;

Methylome analysis and identification of constitutive and stress-specific RNAi-*ddm1* differentially methylated regions (DMRs) and differentially methylated genes (DMGs) in the shoot apical meristem

Global DNA methylation values in the SAM, obtained via HPLC, ranged from 17.5% to 21.3% depending on the line and condition (Fig. S4a), confirming a reduction of whole genome methylation of up to 17.8%, in agreement with Zhu *et al.* (2013). There was no significant line x condition interaction. Values were significantly lower in RNAi-*ddm1* lines compared to the WT under water deficit/rewatering (WD-RW) only, although there was no significant general effect of water deficit (Fig. S4a). Whole genome bisulfite sequencing (WGBS) analysis was performed on SAMs (Fig. S5), and cytosine methylation percentages for the three contexts ranged from 18.6% to 19.6% in the CpG context, 4.4% to 6.0% in the CHG context and 1.6% to 2.0% in the CHH context, with RNAi-*ddm1-15* systematically displaying the lowest values, with a 25.0% decrease for the CHG context (Table S2; Fig. S5d) ;

We considered different types of differentially methylated regions (DMRs) between lines and conditions (Figs 6, S4b, S6a; Tables 1, S3). In order to focus on DMRs specifically related to *PtDDM1* down-regulation, DMRs common to both *ddm1-15* and *ddm1-23* lines vs WT were identified and used for further analysis (Table 1, Fig. 6). In total, 5374 common DMRs were identified under well-watered

conditions (hereafter named 'constitutive RNAi-*ddm1* ' DMRs; Table 1; Figs 6a, S6a). Under the water deficit/rewatering condition, 5172 DMRs were similarly identified, among which 1736 were common to RNAi-*ddm1* constitutive DMRs, while 3436 were specific to the WD-RW condition (hereafter named 'stress-specific RNAi-*ddm1* ' DMRs) (Table 1, Figs 6a, S6a). Altogether, most of the DMRs were hypomethylated and context-dependent, with higher values found in the CHG context, followed by the CpG and CHH contexts (Fig. 6a). However, in the CpG context, these DMRs presented both significant hypo- and hypermethylated patterns (Fig. 6a). In addition, 2592 DMRs that were common to the WT and RNAi-*ddm1* lines were identified in response to water deficit/rewatering (Table 1, Fig. 6b). However, as this type of DMR has already been reported for the WT (Lafon-Placette *et al.*, 2018), we further focused our attention on constitutive and stress-specific RNAi-*ddm1* DMRs (Tables 1, S3; Figs 6, S7).

Regardless of the treatment, constitutive and stress-specific RNAi-*ddm1* DMRs were found in intergenic regions (73% and 71%, for WW and WD-RW conditions, respectively), genes (19% and 21%), promoters ($\pm$ 2 kb from the TSS; 7% and 8%) and TEs (1%, 47 TEs in WW and 48 TEs in WD-RW) (Fig. S7a). Under control conditions, 879 genes were strictly included within the RNAi-*ddm1* constitutive DMRs (hereafter called DMGs for 'differentially methylated genes'), while 910 DMGs were found in stress-specific RNAi-*ddm1* DMRs (Tables 1, S3). Approximately one-third of DMGs (390 genes) were common between conditions and represented constitutive and stable RNAi-*ddm1* -DMGs, while 520 new DMGs were observed (stress-specific RNAi-*ddm1* DMGs) (Tables 1, S3). These numbers increased considerably (up to > 13 000 out of 41 335 genes) when enlarging the windows for DMR identification from 2 kb to 25 kb (Fig. S7b). Under both conditions, a similar number of hypo- and hypermethylated DMGs was found in the CpG context, while in the CHG and CHH contexts, DMGs were mostly hypomethylated (Fig. 6c). In the CHH context, DMGs were slightly methylated (25% to 50% difference) compared to the CpG and CHG contexts (Fig. 6c). Gene ontology (GO) annotation of DMGs (879 in WW or 910 in WD-RW) revealed significant enrichment in similar biological functions such as development (including shoot system morphogenesis), regulation of gene expression (epigenetics, ATP-dependent chromatin remodeling, histone modifications), response to hormones, immune response and abiotic stress (Fig. 6d,e). Under the WD-RW condition, GO terms for the lost DMGs (489, Fig. S7c) were related to development (meristem development), hormones (regulation of hormone levels, response to auxin) and gene silencing. Gene ontology terms for stable DMGs (390, Fig. S7d) were related to development, jasmonic acid, epigenetics, immune response and metabolic processes, while the new DMGs (520, Fig. S7e) were associated with development, and defense/immune/abiotic responses, suggesting that stable and new DMRs preferentially target stress related genes.

In summary, the analysis of the SAM methylome highlighted that *DDM1* knock-down mostly led to hypomethylated CHG DMRs in RNAi-*ddm1* lines, irrespective of the treatment. However, the constitutive *ddm1* -DMRs were largely (approximately two-thirds, Table 1) affected in water deficit conditions (WDRW), suggesting that alteration of *DDM1* machinery in the SAM has the potential to affect development and stress responsive genes, including those related to hormone pathways under stress conditions (Table 1; Fig. S6b).

Transcriptome analysis in the shoot apical meristem

To analyze the impact of a water deficit and rewatering cycle on the SAM, we performed an RNAseq experiment to investigate the differences between RNAi-*ddm1* (*ddm1-23*) and WT SAMs under the WD-RW condition. The identification of differentially expressed genes (DEGs) revealed limited but clear differences (Fig. 7). Out of 32 048 analyzed genes, only 136 genes (Fig. 7; Table S3) were significantly differentially expressed (76 upregulated and 60 down-regulated genes in RNAi-*ddm1* as compared to the WT, $P < 0.05$). Gene ontology annotation revealed significant enrichment in functions such as defense response, immune and wounding responses, response to hormones and signaling, leaf senescence and programmed cell death (Fig. 7a).

The 136 DEGs (RNAi-*ddm1* vs WT in WD-RW condition) were grouped into main classes (Fig. 7b). Genes related to the immune response were systematically up-regulated in RNAi*ddm1* (*RBOHD, CYP94B1, RLP1, RLP56, RPM1, PLDGAMMA1, PDF1*; Fig. 7b). Most genes related to transcription factors (15/17) were also up-regulated (*WRKY, MYB106, ERF, SZF2, PDF2, SVP/AGL22*), with only two genes downregulated (*MYB48* and *DTA2*). Defense and cell wall related genes were both up-regulated (18, including *CHITIV*, *KTI1*, and *PR4*, involved in plant pathogen-interaction) and downregulated (13). Phytohormone pathways were also overrepresented in distinct classes, with 13

DEGs (8 up-regulated and 5 down-regulated) directly involved in defense responsive hormone biosynthetic pathways such as salicylic acid (*SAMTs*), jasmonic acid (*OPR2, CYP94B1*), ethylene (*ERF1, ERF12*), auxin responsive genes (*SAUR29, GH3.1, IBR3, BG1, ABCG36*), gibberellic acid synthesis (*GA3OX1*) and cytokinins (*AHP1*) (Fig. 7b).

Although only seven DEGs overlapped strictly with the DMR genomic locations (previously identified DMGs) (Fig. 7b), 53 were located within the close vicinity of a DMR (± 10 kb) and 98 within ±25 kb (Fig. S8a). Methylation in the three contexts correlated negatively with expression values when considering at least a ± 10 kb window for DMRs (Spearman's *rho* =-0.32 at *P* = 0.0004) (Fig. S8b).

In summary, the analysis of the SAM stress-transcriptome suggests that, under the stress conditions tested, *DDM1* plays a role in repressing genes involved in stress and defense response, including hormonal pathways (Table 1; Fig. S6b).

Mobilome analysis and transposable element genomic integration in the shoot apical meristem

The mobilome-seq approach, which consists of the sequencing of intermediate extrachromosomal circular forms (eccDNA) of TEs (Lanciano *et al.*, 2017), allowed the identification of both active DNA transposons and retrotransposons belonging to 44 to 169 TE families, depending on lines and conditions (RNAi-*ddm1-23* in Fig. 8a, RNAi-*ddm1-15* in Fig. S9a). This number of identified active TE families was always higher under water deficit conditions, regardless of the line. Most of the eccDNAs identified belonged to the annotated *Gypsy, Copia, ENSPM, L1, Ogre, POPGY* and *SAT* families of TEs and repeats. We used depth of coverage (DOC), ranging from 4 x to 51 000 x, to classify TEs into four categories. Transposable elements identified in RNAi*ddm1* and WT lines belonged to the four groups under either condition (Figs 8a, S9a; Table S3), with split-read (SR) coverage ranging from 3 x to 4600 x suggesting the presence of reads spanning the junction of eccDNAs.

Constitutive (WW) and stress-induced (WD-RW) specific TEs were identified (414 TE families in all lines and conditions; Fig. 8a; Table S3). The two most active TEs (*Gypsy*23 and *Gypsy*27) were detected in both WT and RNAi-*ddm1* lines, but *Gypsy*23 was specifically activated under stress conditions (i.e. the WD-RW condition) (Figs 8a, S9a). Active TEs only detected in RNAi-*ddm1* lines were found under WW (28 TEs) and WDRW (89 TEs) conditions. Approximately 21% of the active TEs detected by mobilome-seq strictly co-localized with RNAi-*ddm1* DMRs. This percentage reached > 50% when considering the presence of a DMR at ± 25 kb (Fig. S9b). These active TE families were mainly hypomethylated (*c*. 92% of the TE families) in RNAi-*ddm1* lines (Fig. 8b), and the most active TEs (TE+++) co-localized with DMRs in the CHG context (data not shown). Under stress conditions, active TEs were also hypomethylated in both CpG and CHG contexts but hypermethylated in the CHH context.

The number of genes identified in the vicinity of TEs varied from 45 (TEs inside genes) to 1788 (when considering TEs within ±25 kb of genes) (Fig. S9b; Table S3). Gene ontology annotation of the genes co-localizing with TEs (±10 kb of genes) revealed an enrichment for function in hormone response, immune/defense/abiotic responses and development (Fig. S9c). However, only seven of these genes were previously detected as DEGs (Fig. 7b) when considering the region of ±25 kb.

In order to test for new genomic integrations of the detected active TEs, we assessed copy number variation for three highly active TEs (*DNA-3-3_1, Gypsy23* and *SAT-1*) localized in or near DMRs by qPCR analysis (Figs 8c, S9d). For *DNA-3-3_1*, there was no significant variation in the copy number, regardless of the line and condition. For the other TEs, an increase in copy number was observed in RNAi-*ddm1* lines under water deficit only – 15 copies of *Gypsy*23 in RNAi-*ddm1-23* (Fig. 8c) and 18 copies of *SAT-1* in RNAi-*ddm1-15* (Fig. S9d). In the RNAi-*ddm1* background, *Gypsy*23 is located inside a CHG hypomethylated DMR, while *SAT-1* is found near (2 kb) a CpG and CHG hypomethylated DMR.

In summary, hundreds of active TEs were detected in the SAM, and several of them were stress-induced. *DDM1* knockdown had only a limited impact on the active TE population. However, a genomic copy number increase for two TE families could only be detected in RNAi-*ddm1* lines, showing a role for *DDM1* in protecting meristem genome integrity under stress conditions (Figs 8c, S6b).

DISCUSSION

Relevance of RNAi-*ddm1* poplar lines to the investigation of the stress response in trees

Decreased DNA Methylation I (DDM1) is a plant gene encoding a nucleosome remodeler which facilitates DNA methylation (Zemach *et al.*, 2013; Zhang *et al.*, 2016; Osakabe *et al.*, 2021). While studies on *ddm1* mutants have revealed a major role in silencing TEs and a minor role for *DDM1* on silencing few heterochromatic genes depending on annuals plants (Arabidopsis, tomato, maize, rice), its role in trees and the effect of the environment remain largely unknown (Zemach *et al.*, 2013; Tan *et al.*, 2016; Zhang *et al.*, 2016; Corem *et al.*, 2018; Long *et al.*, 2019). Here, we investigated the role of *DDM1* in a perennial tree (i.e. poplar) under drought conditions in the shoot apical meristem, the center of morphogenesis and differentiation of reproductive cells. We previously characterized stress-induced DMRs in the SAM of various poplars, including the WT *P. tremula* x *P. alba* 717-1B4, revealing that epigenome and transcriptome remodeling following post-drought recovery preferentially affects genes in hormonal pathways (Lafon-Placette *et al.*, 2018). DNA methylation and other epigenetic marks are thought to interact with hormone signaling to control developmental plasticity (Ojolo *et al.*, 2018), especially in meristems (Maury *et al.*, 2019; Amaral *et al.*, 2020) but, so far, functional evidence in meristems has been lacking. Thus, we used a reverse genetic approach and investigated the drought response of RNAi-*ddm1* poplar lines that have already been stabilized *in vitro* for several years (Zhu *et al.*, 2013).

The global hypomethylation observed in the two poplar RNAi-*ddm1* lines indicated that Pt*DDM1* knock-down (Zhu *et al.*, 2013) was effective in the shoot apical meristem. Wholegenome bisulfite sequencing further confirmed this hypomethylation at the genomic level in the three contexts (CpG, CHG and CHH). However, methylation levels in CHG were drastically reduced, suggesting that poplar *DDM1* preferentially targeted methylation in this context. This agrees with reports in rice and maize (Li *et al.*, 2014; Tan *et al.*, 2016; Long *et al.*, 2019) but differs from those in Arabidopsis and tomato (Vongs *et al.*, 1993; Kakutani *et al.*, 1995; Kakutani, 1997; Lippman *et al.*, 2004; Zemach *et al.*, 2013; Corem *et al.*, 2018). In addition, DDM1- dependent methylation in the SAM of poplar was shown to affect active TEs but also many genes, and to be remodeled by the stress conditions. This confirms that the effects of *DDM1* on euchromatic and heterochromatic DNA methylation patterns are different depending on species (Zemach *et al.*, 2013; Tan *et al.*, 2016; Long *et al.*, 2019) and environmental conditions.

The necrotic spots on RNAi-*ddm1* leaves reported by Zhu *et al.* (2013) were consistently observed in our experiment, mainly on mature leaves, and this has previously been associated with *ddm1* mutation in Arabidopsis (Kakutani *et al.*, 1995; Questa € *et al.*, 2013; Kooke *et al.*, 2015) and hypomethylated drm1 drm2 cmt3 mutants (Forgione *et al.*, 2019). It has been suggested that this phenotype is associated with either the demethylation-induced hyperactivation of disease resistance genes or the demethylation-induced reactivation of retrotransposon and virus-like elements under stress conditions (Zhu *et al.*, 2013). In our case, the higher endogenous concentrations of SA observed in the SAM of RNAi-*ddm1* lines would support the first hypothesis, since the accumulation of SA is known to be associated with *DDM1* mutations and is related to the activation of hypersensitive response cell death or systemic acquired resistance (Dong, 2004; Song *et al.*, 2004; Liu *et al.*, 2010; Zhang *et al.*, 2016; Badmi *et al.*, 2019). However, further research in leaves will be needed to confirm this hypothetical SA accumulation in mature leaves in relation to the appearance of necrotic spots during the time-course of the experiment.

Apart from the leaf phenotypic alterations, we did not observe any striking phenotypes for RNAi-*ddm1* lines – growth and water relations under control conditions were mostly comparable to those of the WT. As gas exchanges were measured on young developing leaves without necrotic spots, we do not take into account their potential effect. However, the moderate water deficit revealed subtle differences in growth capability, which, combined with the intrinsic higher cavitation resistance, suggests that alterations to the DDM1-dependent DNA methylation in the two RNAi-*ddm1* lines translated into increased tolerance to water-stress.

Hypomethylated RNAi-*ddm1* poplar lines are more tolerant to water deficit

Tolerance to water deficit is a complex trait encompassing multiple physiological determinants that relate to diverse processes such as growth maintenance, survival, or recovery, depending on the

context of drought intensity and duration (McDowell *et al.*, 2008; Volaire *et al.*, 2018). The moderate water deficit we imposed avoided a rapid growth cessation and promoted steadystate acclimation. The time course of soil REW was similar between the RNAi-*ddm1* and the WT lines during the whole experiment, indicating that all lines actually faced the same level of water deficit. However, while growth progressively slowed in the WT as REW dropped below 40%, as commonly observed in poplars (Bogeat-Triboulot *et al.*, 2007), RNAi-*ddm1* lines remained unaffected. This, combined with the fact that RNAi*ddm1* lines exhibited growth similar to that of the WT under control conditions, suggested increased tolerance to moderate water deficit in the RNAi-*ddm1* lines. Furthermore, the RNAi*ddm1* lines also exhibited higher xylem resistance to droughtinduced cavitation, suggesting improved stress resilience under severe water deficit (Brodribb & Cochard, 2009; Barigah *et al.*, 2013). How modifications to the *DDM1* machinery can affect xylem resistance to cavitation remains unknown at this stage. Interestingly, xylem morphometric features, xylem density and xylem biochemical composition were not significantly different from the WT. However, given the mechanistic understanding of drought-induced cavitation in angiosperms, it is likely that the increased resistance observed in the RNAi-*ddm1* lines was primarily linked to modifications in the ultrastructure of vesselvessel bordered pits (Plavcova & Hacke, 2011; Fichot *et al.*, 2015). Whether the slight gain in intrinsic cavitation resistance (i.e. a few tenths of a MPa) does promote increased survival under severe water deficit, and whether epigenetics might be exploited as such for increasing drought tolerance, remains to be purposely tested.

DDM1-dependent DNA methylation and hormone signaling interact in the shoot apical meristem to orchestrate stress tolerance

The improved stress tolerance in the two RNAi-*ddm1* lines was not associated with sharp differences in water relations or more general phenotypes. Another possibility could be physiological differences related to the phytohormone balance under water deficit. Epigenetics has been linked to phytohormone pathways (Latzel *et al.*, 2012; Yamamuro *et al.*, 2016; Ojolo *et al.*, 2018; Raju *et al.*, 2018; Kooke *et al.*, 2019), which could play a major role in meristems for developmental plasticity (Maury *et al.*, 2019; Amaral *et al.*, 2020). Interestingly, although poplar RNAi-*ddm1* lines displayed hormone profiles in the shoot apex comparable to those of the WT under control conditions, differences were visible under the water deficit conditions, especially for cytokinins (CKs) and salicylic acid (SA). RNAi-*ddm1* lines also displayed decreased expression of histidine-containing phosphotransfer protein 1 (AHP1) which plays a role in propagating cytokinin signal transduction. Cytokinins are known to be negative regulators of stress signaling, and CK-deficient plants with reduced levels of various CKs are generally more tolerant to drought and salt stress (Havlova *et al.*, 2008; Nishiyama *et al.*, 2011; Ha *et al.*, 2012). Higher endogenous levels of SA, as observed for the RNAi-*ddm1* lines compared to WT, have also been shown to promote tolerance to stresses including drought (Munne-Bosch & Penuelas, 2003; Bandurska & Stroi ~ nski, 2005; Azooz & Youssef, 2010; Pandey & Chakraborty, 2015; Sedaghat *et al.*, 2017). Accordingly, SAMT1, a salicylic acid methyltransferase gene, was up-regulated in stressed RNAi-*ddm1* lines compared to the WT (Mofatto *et al.*, 2016).

Although *PtDDM1* knock-down affected the methylation of c. 900 genes common to both RNAi-*ddm1* lines, only a limited number of DEGs was found under water deficit, with seven DEGs strictly overlapping with DMRs (53 for genes at $\pm$10 kb of DMRs). While no clear correlation between DNA methylation and expression changes may exist at the genomic level, the transcriptional activity of a subset of genes still might be regulated, both directly and indirectly, by DNA methylation in response to abiotic stress (Karan *et al.*, 2012; Garg *et al.*, 2015; Chwialkowska *et al.*, 2016; Lafon-Placette *et al.*, 2018). Indeed, we found genes such as transcription factors and hormonerelated pathways that are likely to explain, at least in part, the improved performance of poplar RNAi-*ddm1* lines under water deficit. Several transcription factors, such as *SVP, MYB48, ERF1*, acting in phytohormone pathways and involved in biotic and abiotic stresses were also upregulated in RNAi-*ddm1* lines in comparison to WT under water deficit (Sun & Yu, 2015; Bechtold *et al.*, 2016; He *et al.*, 2016; Wang *et al.*, 2017; Heyman *et al.*, 2018; Wang *et al.*, 2018; Guo *et al.*, 2019). Other DEGs, including genes involved in the leaf cuticle and waxes (*MYB106, CER8, FLA12*), could also partly explain the improved tolerance to moderate water deficit in RNAi-*ddm1* lines by preventing uncontrolled water loss (Chen *et al.*, 2011; Oshima & Mitsuda, 2013, 2016; Wettstein-Knowles, 2016).

Altogether, these findings confirm that common changes in DDM1-dependent DNA methylation found in both RNAi-*ddm1* lines, especially in the shoot apical meristem, can alter hormonal balance and pathways under stress conditions, possibly leading to improved physiological performance (Fig. S6b). This shows the complex connections between chromatin, hormones in meristems and plasticity (Lafon-Placette *et al.*, 2018; Maury *et al.*, 2019).

DDM1-dependent DNA methylation regulates transposable element reactivation and insertion in the shoot apical meristem under stress conditions

The repressive role of DNA methylation and *DDM1* on TE proliferation is well-established in plants (Miura *et al.*, 2001; Johannes *et al.*, 2009; Mirouze *et al.*, 2009; Reinders *et al.*, 2009; Tsukahara *et al.*, 2009; Corem *et al.*, 2018; Quadrana *et al.*, 2019). We identified a large set of active TE families in the SAM, with up to 50% of them located within $\pm$ 25 kb of one RNAi*ddm1* common DMR and being mostly hypomethylated in the CpG and CHG contexts and hypermethylated in the CHH context under stress conditions. However, the activation of TEs was more affected by the stress conditions than the *DDM1* knockdown. We could nonetheless detect increased copy numbers of some of the most active TEs (*Gypsy*-23 and *SAT-1*) only in RNAi-*ddm1* lines under water deficit, suggesting that *DDM1* plays a role in limiting TE reactivation and integration under stressful conditions in the SAM.

Our findings provide evidence that a repression of DDM1dependent DNA methylation can reactivate TEs, especially under stressful conditions, potentially producing genetic variations. Quadrana *et al.* (2019) proposed that TEs are potent and episodic (epi)mutagens that increase the potential for rapid adaptation. Epigenetic regulation may act as a hub through which nongenetically inherited environmentally induced variation in traits can become genetically encoded over generations (Danchin *et al.*, 2019). Recently, Baduel & Colot (2021) proposed that the adaptive contribution of TE-associated epivariations is mainly related to their ability to modulate TE mobilization in response to the environment. This definitely deserves further attention, as genes found close to our active TEs were involved in hormone and stress responses or development. Elucidating the evolutionary significance of both naturally occurring and environmentally induced variations in DNA methylation in the context of tree population dynamics will be of particular interest for long-living organisms such as trees in the age of rapid climate change.

AKNOWLEDGMENTS

MDS and ALLG received PhD grants from the Ministère de la Recherche et Enseignement Superieur. This work was supported by INRAE (grant PI EFPA-2014 to SM), the RTP3E CNRS grants for mobility (http://rtp-3e.wixsite.com/rt3e; ALLG, SM, CG and MM) and access to the IHPE platform (http://galaxy. univ-perp.fr/, Perpignan, France). The LBLGC also benefits from the support of the ANR EPITREE (ANR-17-CE32-0009-01) to SM. English editing was done by Infinity English (no. SIRET 82950710200012). The IJPB benefits from the support of Saclay Plant Sciences-SPS (ANR-17-EUR-0007). This work has benefited from the support of IJPB's Plant Observatory technological platforms. SL and MM were supported by the French National Agency for Research (ANR-13-JSV6-0002 'ExtraChrom') and the Laboratoire d'Excellence LABEX TULIP (ANR-10-LABX-41).

AUTHOR CONTRIBUTIONS

SM designed and coordinated the research. The plant experimental design was established by SM, SHS, RF, and FB. Ecophysiological measurements were performed by A-LLG, RF, AD, ILJ and HC; analysis was conducted by A-LLG and RF. Near infrared spectroscopy (NIRS) measurements and analysis were performed by A-LLG and VS. Phytohormone analysis was performed by SC. DNA and RNA extractions were done by AD, A-LLG and MDS. High-performance liquid chromatography analysis was performed by AD and SM. RNA-seq was conducted and analyzed by JC, VB, and LS-T with MDS. JT and CD performed the WGBS analysis. The WGBS data analysis was performed by SM, ALLG and MDS. Bioinformatics for WGBS was done with the help of CC and CG. Mobilome analysis was performed under the supervision of MM with SL and A-LLG.

Quantitative polymerase chain reaction analyses were performed by MCLD with AD and MDS. Data analysis was performed by SM, A-LLG and MDS. Statistical analyses were performed by RF, A-

LLG and MDS. SM, RF, A-LLG and MDS conceived and wrote the first draft of the manuscript, MM helped revise the manuscript, and SHS edited and helped to direct final analyses and organization of the manuscript. All authors approved the final version of the manuscript. MDS and A-LLG contributed equally to this work.

DATA AVAILABILITY

The data that support the findings of this study are openly available: The WGBS data have been deposited in the Sequence Read Archive (SRA) at https://www.ncbi.nlm.nih.gov/sra/ PRJNA611484, reference no. PRJNA611484; the RNA-Seq data in the GEO (Gene Expression Omnibus) at http://www.ncbi. nlm.nih.gov/geo/query/acc.cgi?acc=GSE135313, reference no. GSE135313 and also in the CATdb database at http://tools.ips2. u-psud.fr/CATdb/, reference no. NGS2017-01-DDM1; and the Mobilome-Seq data in the GEO at https://www.ncbi. nlm.nih.gov/geo/query/acc.cgi?acc=GSE147934, reference no. GSE147934, as well as in the Supporting Information Table S3.

SUPPORTING INFORMATIONS

Additional Supporting Information may be found online in the Supporting Information section at the end of the article.

Fig. S1 Comparison of growth kinetics over the experiment between both conditions.

Fig. S2 Leaf phenotypes among lines under both conditions.

Fig. S3 Physiological differences among lines under both conditions.

Fig. S4 Variations in DNA methylation among RNAi-*ddm1* and wild-type (WT) lines in the shoot apical meristem 1 wk after rewatering (t_2).

Fig. S5 Strategies for bioinformatic analysis of the methylome.

Fig. S6 Concepts and summary of differential methylation analyses: from *ddm1* differentially methylated regions (DMRs) to phenotype.

Fig. S7 Identification of differentially methylated genes (DMGs).

Fig. S8 Relationship between variation in DNA methylation and gene expression.

Fig. S9 Transposable element activity among RNAi-*ddm1* and WT lines in the shoot apical meristem collected 1 wk after rewatering (t_2).

Methods S1 Additional detailed procedures for ecophysiological, genomic and bioinformatic analyses.

Table S1 Xylem structural, functional and biochemical traits measured for the WT and the two RNAi-*ddm1* poplar lines.

Table S2 Mean methylation levels in RNAi-*ddm1* and WT lines in both conditions.

Table S3 Lists of DMRs, DMGs, differentially expressed genes (DEGS), transposable elements (TEs) and genes near TEs. Please note: Wiley Blackwell are not responsible for the content or functionality of any Supporting Information supplied by the authors. Any queries (other than missing material) should be directed to the New Phytologist Central Office.

REFERENCES

Allen CD, Macalady AK, Chenchouni H, Bachelet D, McDowell N, Vennetier M, Kitzberger T, Rigling A, Breshears DD, Hogg EH *et al.* 2010. A global overview of drought and heat-induced tree mortality reveals emerging climate change risks for forests. Forest Ecology and Management 259: 660–684.

AmaralJ, RibeyreZ,VigneaudJ, SowMD, Fichot R, MessierC, Pinto G,Nolet P, MauryS. 2020. Advances andpromises ofepigenetics for forest trees.Forests11: 976.

Anderegg WRL, Klein T, Bartlett M, Sack L, Pellegrini AFA, Choat B, Jansen S. 2016. Meta-analysis reveals that hydraulic traits explain cross-species patterns of drought-induced tree mortality across the globe. Proceedings of the National Academy of Sciences, USA 113: 5024–5029.

Azooz MM, Youssef MM. 2010. Evaluation of heat shock and salicylic acid treatments as inducers of drought stress tolerance in Hassawi wheat. American Journal of Plant Physiology 5: 56–70.

Badmi R, Zhang Y, Tengs T, Brurberg MB, Krokene P, Fossdal CG, Hyt€onen T, Thorstensen T. 2019. Induced and primed defence responses of Fragaria vesca to Botrytis cinerea infection. bioRxiv. doi: 10.1101/692491.

Baduel P, Colot V. 2021. The epiallelic potential of transposable elements and its evolutionary significance in plants. Philosophical Transactions of the Royal Society of London Series B: Biological Sciences 376: 20200123.

Bandurska H, Stroinski A. 2005.The effect of salicylic acid on barley response to water deficit. Acta Physiologiae Plantarum 27: 379–386.

Barigah TS, Charrier O, Douris M, Bonhomme M, Herbette S, Ameglio T, Fichot R, Brignolas F, Cochard H. 2013. Water stress-induced xylem hydraulic failure is a causal factor of tree mortality in beech and poplar. Annals of Botany 112: 1431–1437.

Bechtold U, Penfold CA, Jenkins DJ, Legaie R, Moore JD, Lawson T, Matthews JSA, Vialet-Chabrand SRM, Baxter L, Subramaniam S *et al.* 2016. Time-series transcriptomics reveals that AGAMOUS-LIKE22 affects primary metabolism and developmental processes in drought-stressed Arabidopsis. Plant Cell 28: 345–366.

Bogeat-Triboulot M-B, Brosche M, Renaut J, Jouve L, Thiec DL, Fayyaz P, Vinocur B, Witters E, Laukens K, Teichmann T *et al.* 2007. Gradual soil water depletion results in reversible changes of gene expression, protein profiles, ecophysiology, and growth performance in Populus euphratica, a poplar growing in arid regions. Plant Physiology 143: 876–892.

Bräutigam K, Vining KJ, Lafon-Placette C, Fossdal CG, Mirouze M, Marcos JG, Fluch S, Fraga MF, Guevara MA, Abarca D *et al.* 2013. Epigenetic regulation of adaptive responses of forest tree species to the environment. Ecology and Evolution 3: 399–415.

Brodribb TJ, Cochard H. 2009. Hydraulic failure defines the recovery and point of death in water-stressed conifers. Plant Physiology 149: 575–584.

Carneros E, Yakovlev I, Viejo M, Olsen JE, Fossdal CG. 2017. The epigenetic memory of temperature during embryogenesis modifies the expression of bud burst-related genes in Norway spruce epitypes. Planta 246: 553–566. Chang S, Puryear J, Cairney J. 1993. A simple and efficient method for isolating RNA from pine trees. Plant Molecular Biology Reporter 11: 113–116.

Chen G, Komatsuda T, Ma JF, Li C, Yamaji N, Nevo E. 2011. A functional cutin matrix is required for plant protection against water loss. Plant Signaling & Behavior 6: 1297–1299.

Chwialkowska K, Nowakowska U, Mroziewicz A, Szarejko I, Kwasniewski M. 2016. Water-deficiency conditions differently modulate the methylome of roots and leaves in barley (Hordeum vulgare L.). Journal of Experimental Botany 67: 1109–1121.

Cochard H, Damour G, Bodet C, Tharwat I, Poirier M, Ameglio T. 2005. Evaluation of a new centrifuge technique for rapid generation of xylem vulnerability curves. Physiologia Plantarum 124: 410–418.

Cohen D, Bogeat-Triboulot M-B, Tisserant E, Balzergue S, Martin-Magniette M-L, Lelandais G, Ningre N, Renou J-P, Tamby J-P, Le Thiec D *et al.* 2010. Comparative transcriptomics of drought responses in Populus: a meta-analysis of genome-wide expression profiling in mature leaves and root apices across two genotypes. BMC Genomics 11: 630.

Colome-Tatche M, Cortijo S, Wardenaar R, Morgado L, Lahouze B, Sarazin A, Etcheverry M, Martin A, Feng S, Duvernois-Berthet E *et al.* 2012. Features of the Arabidopsis recombination landscape

resulting from the combined loss of sequence variation and DNA methylation. Proceedings of the National Academy of Sciences, USA 109: 16240–16245.
Corem S, Doron-Faigenboim A, Jouffroy O, Maumus F, Arazi T, Bouche N. 2018. Redistribution of CHH methylation and small interfering RNAs across the genome of tomato *ddm1* mutants. Plant Cell 30: 1628–1644.
Cortijo S, Wardenaar R, Colome-Tatche M, Gilly A, Etcheverry M, Labadie K, Caillieux E, Hospital F, Aury J-m, Wincker P *et al.* 2014. Mapping the epigenetic basis of complex traits. Science 343: 1145–1148.
Danchin E, Pocheville A, Rey O, Pujol B, Blanchet S. 2019. Epigenetically facilitated mutational assimilation: epigenetics as a hub within the inclusive evolutionary synthesis. Biological Reviews 94: 259–282.
Daviaud C, Renault V, Mauger F, Deleuze J-F, Tost J. 2018. Whole-genome bisulfite sequencing using the Ovation® ultralow methyl-seq protocol. Methods in Molecular Biology 1708: 83–104.
Dong X. 2004. NPR1, all things considered. Current Opinion in Plant Biology 7: 547–552.
Doyle JJ, Doyle JL. 1987. A rapid DNA isolation procedure for small quantities of fresh leaf tissue. Phytochemical Bulletin 19: 11–15.
Fichot R, Brignolas F, Cochard H, Ceulemans R. 2015. Vulnerability to drought-induced cavitation in poplars: synthesis and future opportunities. Plant, Cell & Environment 38: 1233–1251.
Forgione I, Wołoszynska M, Pacenza M, Chiappetta A, Greco M, Araniti F, Abenavoli MR, Van Lijsebettens M, Bitonti MB, Bruno L. 2019. Hypomethylated drm1 drm2 cmt3 mutant phenotype of Arabidopsis thaliana is related to auxin pathway impairment. Plant Science 280: 383–396.
Fujimoto R, Sasaki T, Inoue H, Nishio T. 2008. Hypomethylation and transcriptional reactivation of retrotransposon-like sequences in *ddm1* transgenic plants of Brassica rapa. Plant Molecular Biology 66: 463–473.
Fultz D, Choudury SG, Slotkin RK. 2015. Silencing of active transposable elements in plants. Current Opinion in Plant Biology 27: 67–76.
Garg R, Narayana Chevala V, Shankar R, Jain M. 2015. Divergent DNA methylation patterns associated with gene expression in rice cultivars with contrasting drought and salinity stress response. Scientific Reports 5: 14922.
Gömöry D, Hrivnak M, Krajmerova D, Longauer R. 2017. Epigenetic memory effects in forest trees: a victory of “Michurinian biology”? Central European Forestry Journal 63: 173–179.
Gourcilleau D, Bogeat-Triboulot M-B, Le Thiec D, Lafon-Placette C, Delaunay A, El-Soud WA, Brignolas F, Maury S. 2010. DNA methylation and histone acetylation: genotypic variations in hybrid poplars, impact of water deficit and relationships with productivity. Annals of Forest Science 67: 208.
Guo Y, Ping W, Chen J, Zhu L, Zhao Y, Guo J, Huang Y. 2019. Meta-analysis of the effects of overexpression of WRKY transcription factors on plant responses to drought stress. BMC Genetics 20: 63.
Ha S, Vankova R, Yamaguchi-Shinozaki K, Shinozaki K, Tran L-SP. 2012. Cytokinins: metabolism and function in plant adaptation to environmental stresses. Trends in Plant Science 17: 172–179.
Hamanishi ET, Thomas BR, Campbell MM. 2012. Drought induces alterations in the stomatal development program in Populus. Journal of Experimental Botany 63: 4959–4971.
Havlova M, Dobrev PI, Motyka V, Storchova H, Libus J, Dobra J, Malbeck J, Gaudinova A, Vankova R. 2008. The role of cytokinins in responses to water deficit in tobacco plants over-expressing trans-zeatin O-glucosyltransferase gene under 35S or SAG12 promoters. Plant, Cell & Environment 31: 341–353.
He G-H, Xu J-Y, Wang Y-X, Liu J-M, Li P-S, Chen M, Ma Y-Z, Xu Z-S. 2016. Drought-responsive WRKY transcription factor genes TaWRKY1 and TaWRKY33 from wheat confer drought and/or heat resistance in Arabidopsis. BMC Plant Biology 16: 116.
Heyman J, Canher B, Bisht A, Christiaens F, De Veylder L. 2018. Emerging role of the plant ERF transcription factors in coordinating wound defense responses and repair. Journal of Cell Science 131: 208215.
Higo H, Tahir M, Takashima K, Miura A, Watanabe K, Tagiri A, Ugaki M, Ishikawa R, Eiguchi M, Kurata N *et al.* 2012. *DDM1* (Decrease in DNA Methylation) genes in rice (Oryza sativa). Molecular Genetics and Genomics 287: 785–792.

Ikeda Y, Nishimura T. 2015. The role of DNA methylation in transposable element silencing and genomic imprinting. In: Nuclear Functions in Plant Transcription, Signaling and Development. New York, NY, USA: Springer, 13– 29.

Ito T, Tarutani Y, To TK, Kassam M, Duvernois-Berthet E, Cortijo S, Takashima K, Saze H, Toyoda A, Fujiyama A *et al.* 2015. Genome-wide negative feedback drives transgenerational DNA methylation dynamics in Arabidopsis. PLoS Genetics 11: e1005154.

Jansson S, Douglas CJ. 2007. Populus: a model system for plant biology. Annual Review of Plant Biology 58: 435–458.

Johannes F, Porcher E, Teixeira FK, Saliba-Colombani V, Simon M, Agier N, Bulski A, Albuisson J, Heredia F, Audigier P *et al.* 2009. Assessing the impact of transgenerational epigenetic variation on complex traits. PLoS Genetics 5: e1000530.

Kakutani T. 1997. Genetic characterization of late-flowering traits induced by DNA hypomethylation mutation in Arabidopsis thaliana. The Plant Journal 12: 1447–1451.

Kakutani T, Jeddeloh JA, Richards EJ. 1995. Characterization of an Arabidopsis thaliana DNA hypomethylation mutant. Nucleic Acids Research 23: 130– 137.

Karan R, DeLeon T, Biradar H, Subudhi PK. 2012. Salt stress induced variation in DNA methylation pattern and its influence on gene expression in contrasting rice genotypes. PLoS ONE 7: e40203.

Kawanabe T, Ishikura S, Miyaji N, Sasaki T, Wu LM, Itabashi E, Takada S, Shimizu M, Takasaki-Yasuda T, Osabe K *et al.* 2016. Role of DNA methylation in hybrid vigor in Arabidopsis thaliana. Proceedings of the National Academy of Sciences, USA 113: E6704–E6711.

Kooke R, Johannes F, Wardenaar R, Becker F, Etcheverry M, Colot V, Vreugdenhil D, Keurentjes JJB. 2015. Epigenetic basis of morphological variation and phenotypic plasticity in Arabidopsis thaliana. Plant Cell Online 27: 337–348.

Kooke R, Morgado L, Becker F, van Eekelen H, Hazarika R, Zheng Q, de Vos RCH, Johannes F, Keurentjes JJB. 2019. Epigenetic mapping of the Arabidopsis metabolome reveals mediators of the epigenotype-phenotype map. Genome Research 29: 96–106.

Lafon-Placette C, Faivre-Rampant P, Delaunay A, Street N, Brignolas F, Maury S. 2013. Methylome of DNase I sensitive chromatin in Populus trichocarpa shoot apical meristematic cells: a simplified approach revealing characteristics of gene-body DNA methylation in open chromatin state. New Phytologist 197: 416–430.

Lafon-Placette C, Le Gac A-L, Chauveau D, Segura V, Delaunay A, LesageDescauses M-C, Hummel I, Cohen D, Jesson B, Le Thiec D *et al.* 2018. Changes in the epigenome and transcriptome of the poplar shoot apical meristem in response to water availability affect preferentially hormone pathways. Journal of Experimental Botany 69: 537–551.

Lanciano S, Carpentier M-C, Llauro C, Jobet E, Robakowska-Hyzorek D, Lasserre E, Ghesquiere A, Panaud O, Mirouze M. 2017. Sequencing the extrachromosomal circular mobilome reveals retrotransposon activity in plants. PLoS Genetics 13: e1006630.

Latzel V, Zhang Y, Karlsson Moritz K, Fischer M, Bossdorf O. 2012. Epigenetic variation in plant responses to defence hormones. Annals of Botany 110: 1423– 1428.

Le Gac A-L, Lafon-Placette C, Chauveau D, Segura V, Delaunay A, Fichot R, Marron N, Le Jan I, Berthelot A, Bodineau G *et al.* 2018. Winter-dormant shoot apical meristem in poplar trees shows environmental epigenetic memory. Journal of Experimental Botany 69: 4821–4837.

Le Gac A-L, Lafon-Placette C, Delaunay A, Maury S. 2019. Developmental, genetic and environmental variations of global DNA methylation in the first leaves emerging from the shoot apical meristem in poplar trees. Plant Signaling & Behavior 14: 1596717.

Li Q, Eichten SR, Hermanson PJ, Springer NM. 2014. Inheritance patterns and stability of DNA methylation variation in maize near-isogenic lines. Genetics 196: 667–676.

Liang D, Zhang Z, Wu H, Huang C, Shuai P, Ye C-Y, Tang S, Wang Y, Yang L, Wang J *et al.* 2014. Single-base-resolution methylomes of Populus trichocarpa reveal the association between DNA methylation and drought stress. BMC Genetics 15: S9.

Li-Marchetti C, Le Bras C, Relion D, Citerne S, Huche-Thelier L, Sakr S, Morel P, Crespel L. 2015. Genotypic differences in architectural and physiological responses to water restriction in rose bush. Frontiers in Plant Science 6: 1–14.

Lippman Z, Gendrel A-V, Black M, Vaughn MW, Dedhia N, Richard McCombie W, Lavine K, Mittal V, May B, Kasschau KD *et al.* 2004. Role of transposable elements in heterochromatin and epigenetic control. Nature 430: 471–476.

Liu G, Ji Y, Bhuiyan NH, Pilot G, Selvaraj G, Zou J, Wei Y. 2010. Amino acid homeostasis modulates salicylic acid-associated redox status and defense responses in Arabidopsis. Plant Cell 22: 3845–3863.

Long JC, Xia AA, Liu JH, Jing JL, Wang YZ, Qi CY, He Y. 2019. Decrease in DNA methylation 1 (DDM1) is required for the formation of mCHH islands in maize. Journal of Integrative Plant Biology 61: 749–764.

Maury S, Sow MD, Le Gac A-L, Genitoni J, Lafon-Placette C, Mozgova I. 2019. Phytohormone and chromatin crosstalk: The missing link for developmental plasticity? Frontiers in Plant Science 10: 395.

McDowell N, Pockman WT, Allen CD, Breshears DD, Cobb N, Kolb T, Plaut J, Sperry J, West A, Williams DG *et al.* 2008. Mechanisms of plant survival and mortality during drought: why do some plants survive while others succumb to drought? New Phytologist 178: 719–739.

Mirouze M, Paszkowski J. 2011. Epigenetic contribution to stress adaptation in plants. Current Opinion in Plant Biology 14: 267–274.

Mirouze M, Reinders J, Bucher E, Nishimura T, Schneeberger K, Ossowski S, Cao J, Weigel D, Paszkowski J, Mathieu O. 2009. Selective epigenetic control of retrotransposition in Arabidopsis. Nature 461: 427–430.

Miura A, Yonebayashi S, Watanabe K, Toyama T, Shimada H, Kakutani T. 2001. Mobilization of transposons by a mutation abolishing full DNA methylation in Arabidopsis. Nature 411: 212–214.

Mofatto LS, Carneiro FdA, Vieira NG, Duarte KE, Vidal RO, Alekcevetch JC, Cotta MG, Verdeil J-L, Lapeyre-Montes F, Lartaud M *et al.* 2016. Identification of candidate genes for drought tolerance in coffee by highthroughput sequencing in the shoot apex of different Coffea arabica cultivars. BMC Plant Biology 16: 94.

Monclus R, Dreyer E, Villar M, Delmotte FM, Delay D, Petit J-M, Barbaroux C, Le Thiec D, Brechet C, Brignolas F. 2006. Impact of drought on productivity and water use efficiency in 29 genotypes of Populus deltoides9Populus nigra. New Phytologist 169: 765–777.

Munne-Bosch S, Penuelas J. 2003.~ Photo- and antioxidative protection, and a role for salicylic acid during drought and recovery in field-grown Phillyrea angustifolia plants. Planta 217: 758–766.

Nishiyama R, Watanabe Y, Fujita Y, Le DT, Kojima M, Werner T, Vankova R, Yamaguchi-Shinozaki K, Shinozaki K, Kakimoto T *et al.* 2011. Analysis of cytokinin mutants and regulation of cytokinin metabolic genes reveals important regulatory roles of cytokinins in drought, salt and abscisic acid responses, and abscisic acid biosynthesis. Plant Cell 23: 2169–2183.

Ojolo SP, Cao S, Priyadarshani SVGN, Li W, Yan M, Aslam M, Zhao H, Qin Y. 2018. Regulation of plant growth and development: A review from a chromatin remodeling perspective. Frontiers in Plant Science 9: 1232.

Osakabe A, Jamge B, Axelsson E, Montgomery SA, Akimcheva S, Kuehn AL, Pisupati R, Lorkovic ZJ, Yelagandula R, Kakutani T *et al.* 2021. The chromatin remodeler *DDM1* prevents transposon mobility through deposition of histone variant H2A.W. Nature Cell Biology 23: 391–400.

Oshima Y, Mitsuda N. 2013. The MIXTA-like Transcription factor MYB16 is a major regulator of cuticle formation in vegetative organs. Plant Signaling & Behavior 8: e26826.

Oshima Y, Mitsuda N. 2016. Enhanced cuticle accumulation by employing MIXTA-like transcription factors. Plant Biotechnology 33: 161–168.

Pandey S, Chakraborty D. 2015. Salicylic acid and drought stress response: Biochemical to molecular crosstalk. In: Tripathi BN, Muller M, eds.€ Stress responses in plants: Mechanisms of toxicity and tolerance. Cham, Switzerland: Springer International Publishing, 247–265.

Plavcova L, Hacke UG. 2011. Heterogeneous distribution of pectin epitopes and calcium in different pit types of four angiosperm species. New Phytologist 192: 885–897.

Plomion C, Bastien C, Bogeat-Triboulot M-B, Bouffier L, Dejardin A, Duplessis S, Fady B, Heuertz M, Le Gac A-L, Le Provost G *et al.* 2016. Forest tree genomics: 10 achievements from the past 10 years and future prospects. Annals of Forest Science 73: 77–103.

Quadrana L, Etcheverry M, Gilly A, Caillieux E, Madoui M-A, Guy J, Bortolini Silveira A, Engelen S, Baillet V, Wincker P *et al.* 2019. Transposition favors the generation of large effect mutations that may facilitate rapid adaption. Nature Communications 10: 1–10.

Questa JI, Fina JP, Casati P. 2013.€ *DDM1* and ROS1 have a role in UV-B induced- and oxidative DNA damage in A. thaliana. Frontiers in Plant Science 4: 420.

R Development Core Team. 2015. R: A language and environment for statistical computing. Vienna, Austria: R Foundation for Statistical Computing.

Raj S, Br€autigam K, Hamanishi ET, Wilkins O, Thomas BR, Schroeder W, Mansfield SD, Plant AL, Campbell MM. 2011. Clone history shapes Populus drought responses. Proceedings of the National Academy of Sciences, USA 108: 12521–12526.

Raju SKK, Shao M-R, Sanchez R, Xu Y-Z, Sandhu A, Graef G, Mackenzie S. 2018. An epigenetic breeding system in soybean for increased yield and stability. Plant Biotechnology Journal 16: 1836–1847.

Reinders J, Wulff BBH, Mirouze M, Marı-Ordonez A, Dapp M, Rozhon W,~ Bucher E, Theiler G, Paszkowski J. 2009. Compromised stability of DNA methylation and transposon immobilization in mosaic Arabidopsis epigenomes. Genes & Development 23: 939–950.

Russo VEA, Riggs AD, Martienssen RA. 1996. Epigenetic mechanisms of gene regulation. Cold Spring Harbour, NY, USA: Cold Spring Harbour Laboratory Press.

Sasaki T, Kobayashi A, Saze H, Kakutani T. 2012. RNAi-independent de novo DNA methylation revealed in Arabidopsis mutants of chromatin remodeling gene DDM1. The Plant Journal 70: 750–758.

Saze H, Kakutani T. 2007. Heritable epigenetic mutation of a transposonflanked Arabidopsis gene due to lack of the chromatin-remodeling factor DDM1. EMBO Journal 26: 3641–3652.

Schmid MW, Giraldo-Fonseca A, R€ovekamp M, Smetanin D, Bowman JL, Grossniklaus U. 2018. Extensive epigenetic reprogramming during the life cycle of Marchantia polymorpha. Genome Biology 19: 9.

Sedaghat M, Tahmasebi-Sarvestani Z, Emam Y, Mokhtassi-Bidgoli A. 2017. Physiological and antioxidant responses of winter wheat cultivars to strigolactone and salicylic acid in drought. Plant Physiology and Biochemistry 119: 59–69.

Slotkin RK, Martienssen R. 2007. Transposable elements and the epigenetic regulation of the genome. Nature Reviews Genetics 8: 272–285.

Song JT, Lu H, McDowell JM, Greenberg JT. 2004. A key role for ALD1 in activation of local and systemic defenses in Arabidopsis. The Plant Journal 40: 200–212.

Sow MD, Allona I, Ambroise C, Conde D, Fichot R, Gribkova S, Jorge V, LeProvost G, P^aques L, Plomion C *et al.* 2018a. Epigenetics in Forest Trees. In:Bucher E, Gallusci P, Mirouze M, eds. Advances in botanical research. London, UK: Academic Press, 387–453.

Sow MD, Segura V, Chamaillard S, Jorge V, Delaunay A, Lafon-Placette C, Fichot R, Faivre-Rampant P, Villar M, Brignolas F *et al.* 2018b. Narrowsense heritability and PST estimates of DNA methylation in three Populus nigra L. populations under contrasting water availability. Tree Genetics & Genomes 14: 78.

Street NR, Skogstr€om O, Sj€odin A, Tucker J, Rodrıguez-Acosta M, Nilsson P, Jansson S, Taylor G. 2006. The genetics and genomics of the drought response in Populus. The Plant Journal 48: 321–341.

Sun Y, Yu D. 2015. Activated expression of AtWRKY53 negatively regulates drought tolerance by mediating stomatal movement. Plant Cell Reports 34: 1295–1306.

Tan F, Zhou C, Zhou Q, Zhou S, Yang W, Zhao Y, Li G, Zhou D-X. 2016. Analysis of chromatin regulators reveals specific features of rice DNA methylation pathways. Plant Physiology 171: 2041–2054.

Trapet P, Avoscan L, Klinguer A, Pateyron S, Citerne S, Chervin C, Mazurier S, Lemanceau P, Wendehenne D, Besson-Bard A. 2016. The Pseudomonas fluorescens siderophore pyoverdine weakens Arabidopsis thaliana defense in favor of growth in iron-deficient conditions. Plant Physiology 171: 675–693.

Tsukahara S, Kobayashi A, Kawabe A, Mathieu O, Miura A, Kakutani T. 2009. Bursts of retrotransposition reproduced in Arabidopsis. Nature 461: 423–426.

Tuskan GA, DiFazio S, Jansson S, Bohlmann J, Grigoriev I, Hellsten U, Putnam N, Ralph S, Rombauts S, Salamov A *et al.* 2006. The genome of Black Cottonwood, Populus trichocarpa (Torr. & Gray). Science 313: 1596– 1604.

Vining KJ, Pomraning KR, Wilhelm LJ, Priest HD, Pellegrini M, Mockler TC, Freitag M, Strauss SH. 2012. Dynamic DNA cytosine methylation in the Populus trichocarpa genome: tissue-level variation and relationship to gene expression. BMC Genomics 13: 27.

Volaire F, Lens F, Cochard H, Xu H, Chacon-Doria L, Bristiel P, Balachowski J, Rowe N, Violle C, Picon-Cochard C. 2018. Embolism and mechanical resistances play a key role in dehydration tolerance of a perennial grass Dactylis glomerata L. Annals of Botany 122: 325–336.

Vongs A, Kakutani T, Martienssen RA, Richards EJ. 1993. Arabidopsis thaliana DNA methylation mutants. Science 260: 1926–1928.

Wang Y, Wang Q, Liu M, Bo C, Wang X, Ma Q, Cheng B, Cai R. 2017. Overexpression of a maize MYB48 gene confers drought tolerance in transgenic Arabidopsis plants. Journal of Plant Biology 60: 612–621.

Wang Z, Wang F, Hong Y, Yao J, Ren Z, Shi H, Zhu J-K. 2018. The flowering repressor SVP confers drought resistance in Arabidopsis by regulating abscisic acid catabolism. Molecular Plant 11: 1184–1197.

Wasserstein RL, Lazar NA. 2016. The ASA statement on p-Values: context, process, and purpose. The American Statistician 70: 129–133.

von Wettstein-Knowles P. 2016. Plant waxes. In: eLS. Chichester, UK: John Wiley & Sons, American Cancer Society, 1–13.

Yakovlev IA, Carneros E, Lee Y, Olsen JE, Fossdal CG. 2016. Transcriptional profiling of epigenetic regulators in somatic embryos during temperature induced formation of an epigenetic memory in Norway spruce. Planta 243: 1237–1249.

Yakovlev I, Fossdal CG, Skrøppa T, Olsen JE, Jahren AH, Johnsen Ø. 2012. An adaptive epigenetic memory in conifers with important implications for seed production. Seed Science Research 22: 63–76.

Yakovlev IA, Fossdal CG. 2017. In silico analysis of small RNAs suggest roles for novel and conserved miRNAs in the formation of epigenetic memory in somatic embryos of Norway spruce. Frontiers in Physiology 8: 674.

Yakovlev IA, Lee Y, Rotter B, Olsen JE, Skrøppa T, Johnsen Ø, Fossdal CG. 2014. Temperature-dependent differential transcriptomes during formation of an epigenetic memory in Norway spruce embryogenesis. Tree Genetics & Genomes 10: 355–366.

Yamamuro C, Zhu J-K, Yang Z. 2016. Epigenetic modifications and plant hormone action. Molecular Plant 9: 57–70.

Yao Y, Bilichak A, Golubov A, Kovalchuk I. 2012. *ddm1* plants are sensitive to methyl methane sulfonate and NaCl stresses and are deficient in DNA repair. Plant Cell Reports 31: 1549–1561.

Zemach A, Kim MY, Hsieh P-H, Coleman-Derr D, Eshed-Williams L, Thao K, Harmer SL, Zilberman D. 2013. The Arabidopsis nucleosome remodeler *DDM1* allows DNA methyltransferases to access H1-containing heterochromatin. Cell 153: 193–205.

Zhang H, Lang Z, Zhu J-K. 2018a. Dynamics and function of DNA methylation in plants. Nature Reviews Molecular Cell Biology 19: 489–506.

Zhang Q, Li Y, Xu T, Srivastava AK, Wang D, Zeng L, Yang L, He Li, Zhang H, Zheng Z *et al.* 2016. The chromatin remodeler *DDM1* promotes hybrid vigor by regulating salicylic acid metabolism. Cell Discovery 2: 16027.

Zhang Y-Y, Latzel V, Fischer M, Bossdorf O. 2018b. Understanding the evolutionary potential of epigenetic variation: a comparison of heritable phenotypic variation in epiRILs, RILs, and natural ecotypes of Arabidopsis thaliana. Heredity 121: 257–265.

Zhou Y, Zhou B, Pache L, Chang M, Khodabakhshi AH, Tanaseichuk O, Benner C, Chanda SK. 2019. Metascape provides a biologist-oriented resource for the analysis of systems-level datasets. Nature Communications 10: 1523.

Zhu R, Shevchenko O, Ma C, Maury S, Freitag M, Strauss SH. 2013. Poplars with a PtDDM1-RNAi transgene have reduced DNA methylation and show aberrant post-dormancy morphology. Planta 237: 1483–1493.

Fig. 1

General overview of the drought experiment on poplars (*Populus tremula* x *Populus alba*). (a) Timeline of the experiment. Propagated *in vitro* plantlets from the wild-type (WT) and the two RNAi*ddm1* transgenic lines were acclimated in a heated glasshouse, transferred into 4 l pots and kept under control conditions until they were 3-months-old. At that time (t_0), a water deficit was initiated for the plants assigned to the water deficit/rewatering treatment (WDRW), while control plants were kept wellwatered (WW). After 3 wk of water deficit (t_1), plants of the WD-RW condition were rewatered to field capacity for 1 wk, after which the experiment ended (t_2). The ecophysiological characterization of plant material was performed between t_0 and t_2. Sampling of shoot apical meristems (SAMs) for molecular analysis was performed at t2. (b) Overview of the plants in the glasshouse. (c) Examples of plant phenotypes at t2 under WW and WD-RW conditions for WT and RNAi-*ddm1* lines.

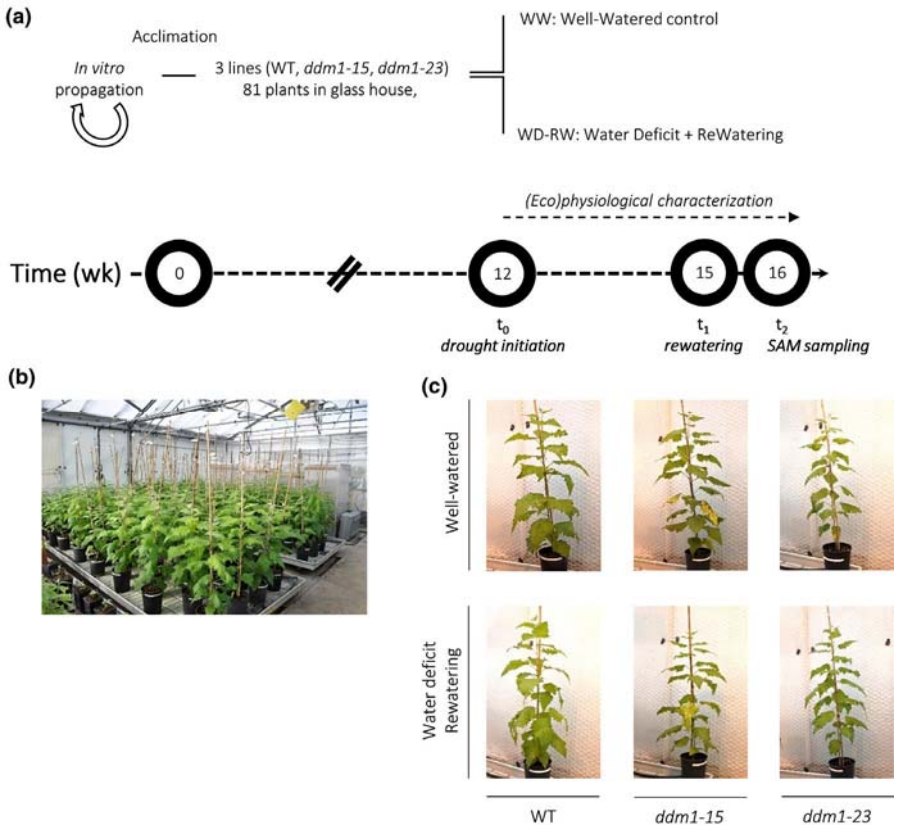

Fig. 2

Measurements of soil water content and leaf water potential during the experiment. (a) Time course of soil relative extractable water (REW) during the experiment for the wild-type (WT) and the two RNAi-*ddm1* (*ddm1-15*, *ddm1-23*) transgenic poplar lines (*Populus tremula* x *Populus alba*) under control (well-watered, WW) and stress (moderate water deficit followed by rewatering, WD-RW) conditions. Water deficit in the WD-RW condition started on day 0 (t_0) and lasted for 3 wk, after which plants were rewatered (t_1) for an additional 1 wk period (t_2). Values are genotypic means ±SE (n = 6 for WW, n = 12 for WD-RW). (b) Predawn leaf water potential measured at the drought peak (i.e. before rewatering on day 21) for the WT and the two RNAi-*ddm1* (*ddm1-15*, *ddm1-23*) poplar lines. The white bars represent the control condition and the black bars represent the stress condition (moderate water deficit followed by rewatering). Values are genotypic means ±SE (n = 5). Asterisks indicate significant differences between conditions for each line (***, P < 0.001)

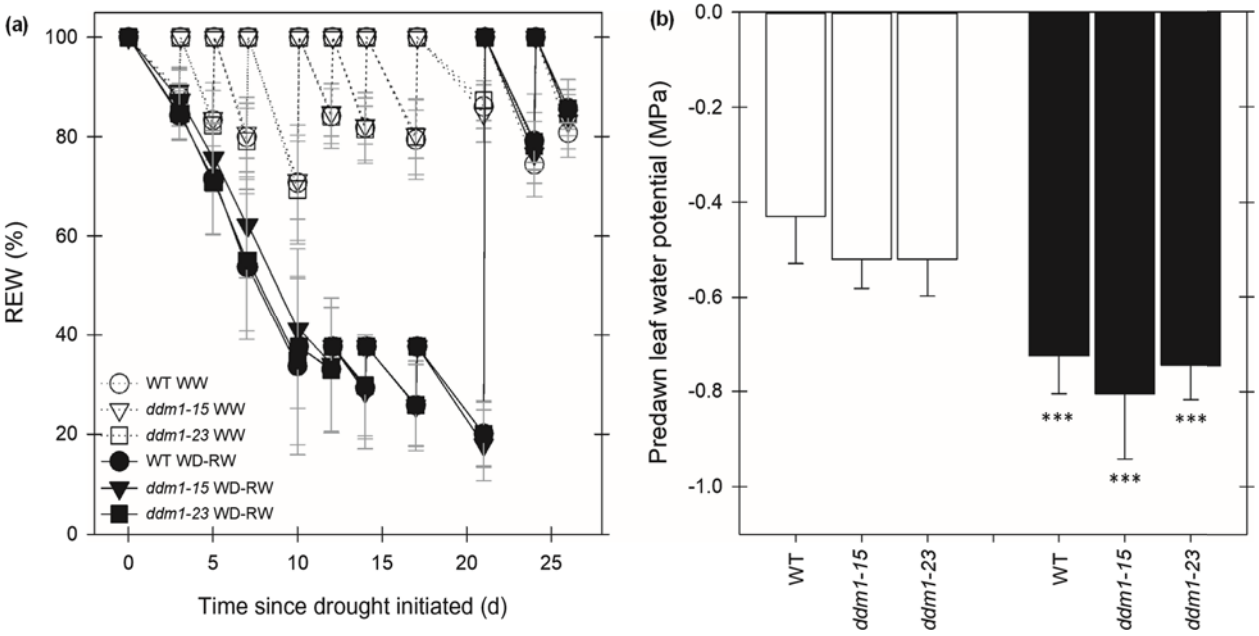

Fig. 3

Physiological traits measured during the drought experiment. (a) Height and (b) diameter growth rates during the 3 wk of water deficit from t0 to t1 for the wild-type (WT) and the two RNAi-*ddm1* (*ddm1-15*, *ddm1-23*) poplar lines (*Populus tremula* x *Populus alba*). The white bars represent the well-watered condition (WW) and the black bars represent the stress condition (moderate water deficit followed by rewatering, WD-RW). Values are means ±SE (*n* = 6 per line for WW, *n* = 12 per line for WD-RW). The effects of water deficit were evaluated for each line using a ttest and differences are only indicated if significant (*, $P < 0.05$). Statistical tests did not reveal significant differences between lines when considering conditions separately, but the WT was the only line to be significantly affected by water deficit. (c) Average xylem vulnerability curves for the WT and the two RNAi-*ddm1* (*ddm1-15*, *ddm1-23*) poplar lines. PLC, percent loss of hydraulic conductance. Measurements were performed at t_2 on well-watered plants only. Values are means ±SE (*n* = 6 per line).

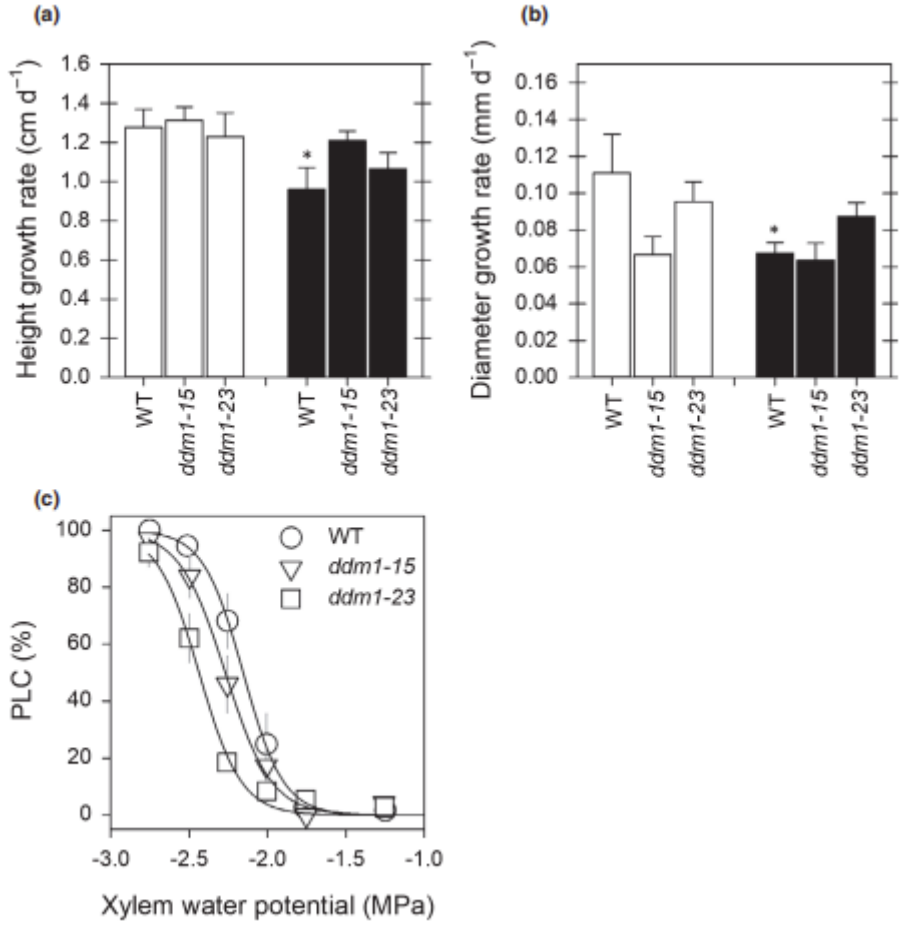

Fig. 4

Leaf phenotypes during the drought experiment. Plants were phenotyped for the occurrence of (a) necrotic spots (mottled phenotype) and (b) folded phenotype. For each panel the upper part shows a picture of a typical phenotype, and the lower graph shows a time course of leaf phenotypic alterations for the wild-type (WT) and the two RNAi-*ddm1* (*ddm1-15*, *ddm1-23*) poplar lines (*Populus tremula* x *Populus alba*) under control (well-watered, WW) and stress (moderate water deficit followed by rewatering, WD-RW) conditions. Values are line means ±SE (*n* = 6 for WW, *n* = 12 for WD-RW). At the end of the experiment (t2), all lines differed significantly from each other for the proportion of necrotic spots (mottled phenotype), but water deficit had no significant effect; only *ddm1-23* showed a significantly higher proportion of folded leaves, but water deficit still had no significant effect

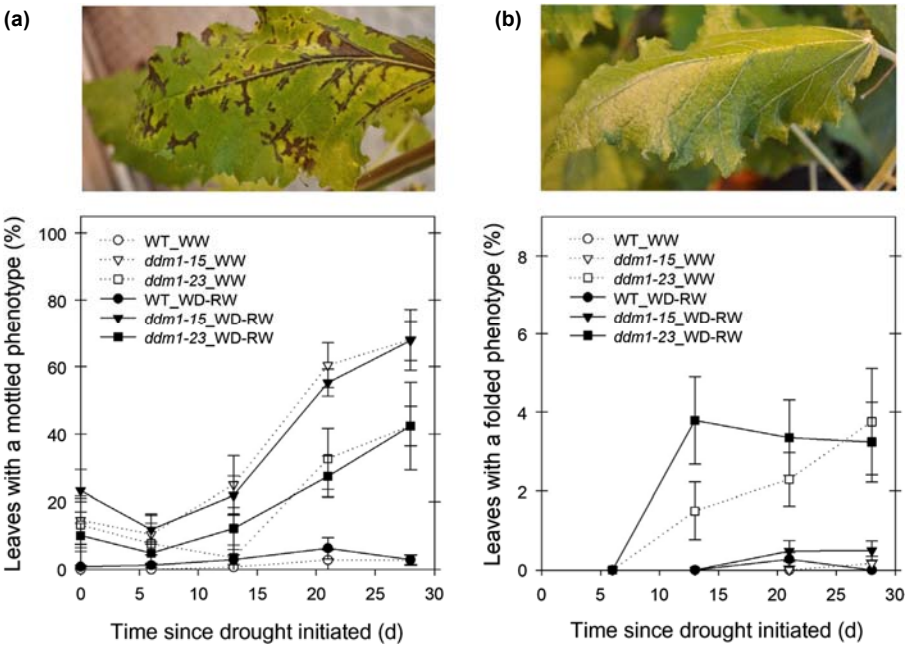

Fig. 5

Phytohormone content in the shoot apical meristems. Measurements were performed at rewatering (t_1) for the wildtype (WT) and the two RNAi-*ddm1* (*ddm1-15*, *ddm1-23*) poplar lines (*Populus tremula* x *Populus alba*) for the six indicated phytohormones. White bars represent the control condition (WW) and white bars represent the stress condition (moderate water deficit followed by rewatering, WDRW). Values are genotypic means ±SE (n = 3). The effects of water deficit were evaluated within each line using a t-test and differences are only indicated when significant (*, $P < 0.05$; **, $P < 0.01$; ***, $P < 0.001$). Different letters indicate significant differences between lines within each condition (uppercase for WW, lowercase for WD-RW) following a Tukey's post-hoc test. The dashed lines indicate the detection threshold for each phytohormone.

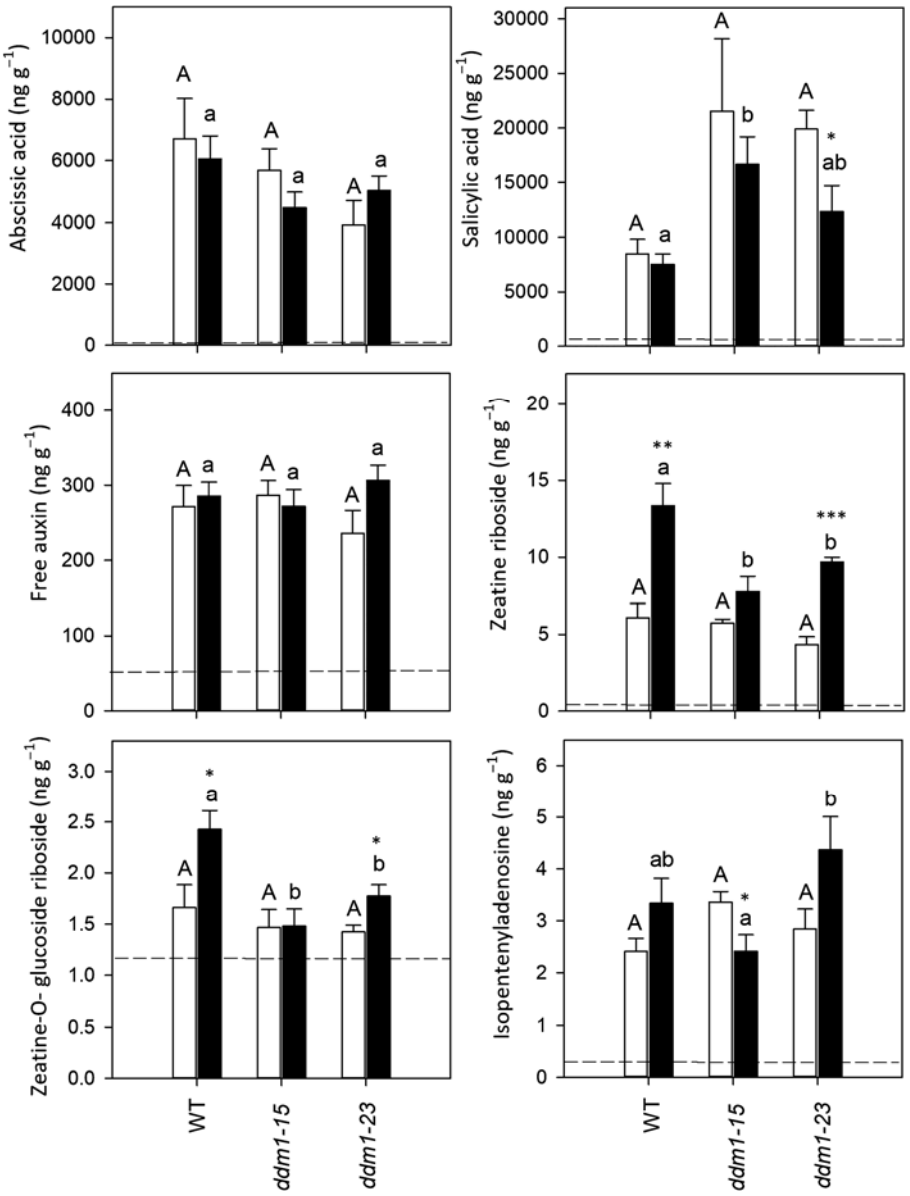

Fig. 6

Variations in DNA methylation among RNAi-*ddm1* and wild-type (WT) lines in shoot apical meristems 1 wk after rewatering (t_2). (a) Common differentially methylated regions (DMRs) between the two RNAi-*ddm1* lines (*ddm1-15* and *ddm1-23*) (*Populus tremula* x *Populus alba*) vs the WT in all sequence contexts (CpG, CHG and CHH) under well-watered (WW) and stress (moderate water deficit followed by rewatering, WD-RW) conditions. Black bars represent hypomethylated DMRs and grey bars represent hypermethylated DMRs. (b) Identification of DMRs in WD-RW conditions compared to WW conditions for WT and RNAi-*ddm1* lines. Black bars represent hypomethylated DMRs and grey bars represent hypermethylated DMRs. (c) Genic DNA methylation variation of the common DMRs in the RNAi-*ddm1* lines vs the WT line under WW and WD-RW conditions for each methylation context. Only DMRs with at least a 25% difference were kept, except for CHH where a threshold of 10% was applied due to the low proportion of DMRs in that context. (d) Heatmap view of enriched clusters on constitutive (i.e. not stress induced) RNAi-*ddm1* differentially methylated genes (DMGs) (in WW) (*n* = 879 annotations of homologous Arabidopsis genes). Each bar is a single cluster representative of TAIR10 corresponding to sPta717 v1.1 annotations. (e) Heatmap view of enriched clusters on stress-specific RNAi-*ddm1* DMGs (in WD-RW) (*n* = 910 annotations of homologous Arabidopsis genes). Enriched GO clusters were generated using METASCAPE (Zhou *et al.*, 2019; see Supporting Information Methods S1).

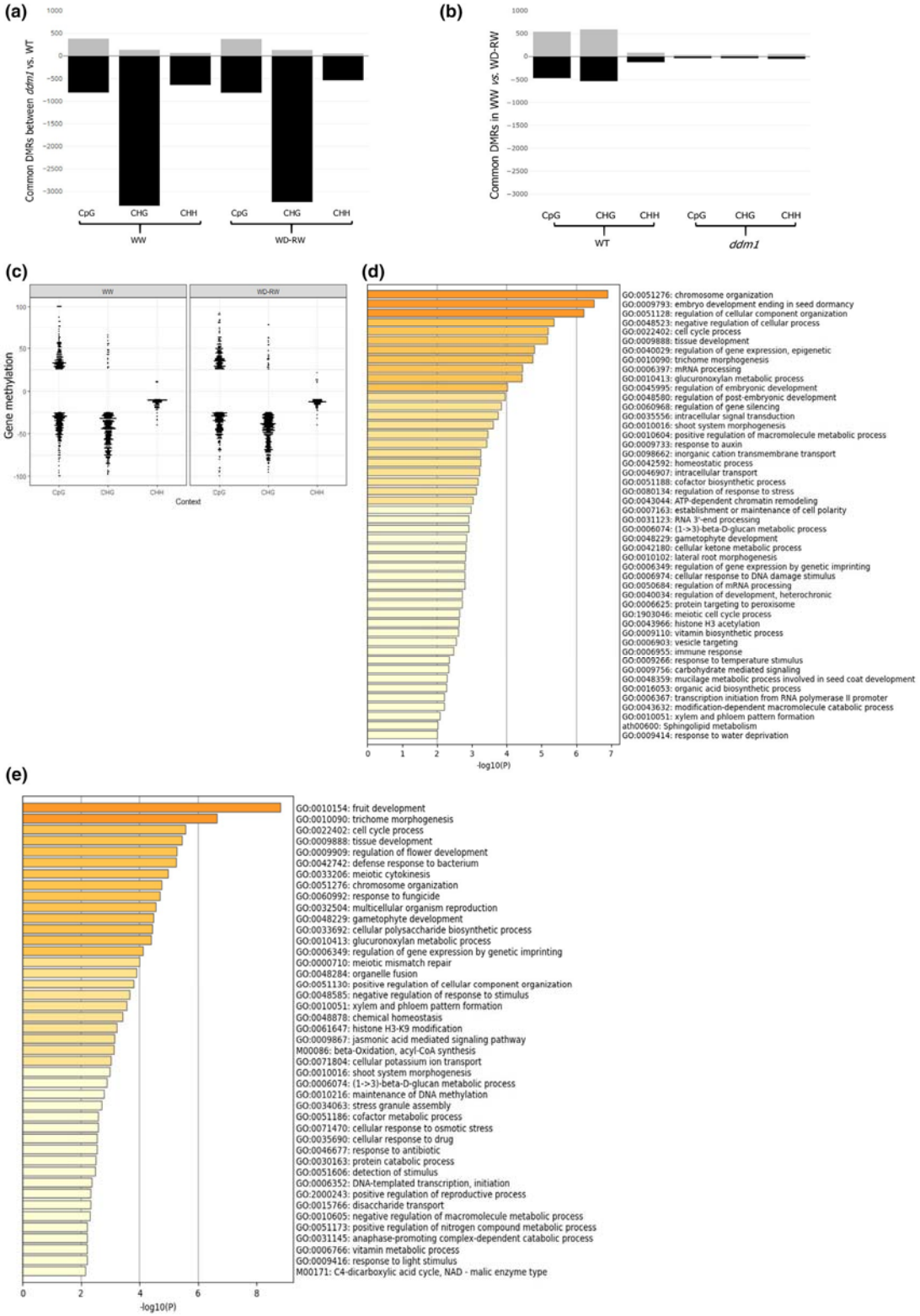
(a)
Common DMRs between ddm1 vs. WT
1000
500
0
−500
−1000
−1500
−2000
−2500
−3000
CpG
CHG
CHH
CpG
CHG
CHH
WW
WD-RW
(b)
Common DMRs in WW vs. WD-RW
1000
500
0
−500
−1000
−1500
−2000
−2500
−3000
CpG
CHG
CHH
CpG
CHG
CHH
WT
ddm1
(c)
WW
WD-RW
Gene methylation
100
50
0
-50
-100
CpG
CHG
CHH
CpG
CHG
CHH
Context
(d)
GO:0051276: chromosome organization
GO:0009793: embryo development ending in seed dormancy
GO:0051128: regulation of cellular component organization
GO:0048523: negative regulation of cellular process
GO:0022402: cell cycle process
GO:0009888: tissue development
GO:0040029: regulation of gene expression, epigenetic
GO:0010090: trichome morphogenesis
GO:0006397: mRNA processing
GO:0010413: glucuronoxylan metabolic process
GO:0045995: regulation of embryonic development
GO:0048580: regulation of post-embryonic development
GO:0060968: regulation of gene silencing
GO:0035556: intracellular signal transduction
GO:0010016: shoot system morphogenesis
GO:0010604: positive regulation of macromolecule metabolic process
GO:0009733: response to auxin
GO:0098662: inorganic cation transmembrane transport
GO:0042592: homeostatic process
GO:0046907: intracellular transport
GO:0051188: cofactor biosynthetic process
GO:0080134: regulation of response to stress
GO:0043044: ATP-dependent chromatin remodeling
GO:0007163: establishment or maintenance of cell polarity
GO:0031123: RNA 3'-end processing
GO:0006074: (1->3)-beta-D-glucan metabolic process
GO:0048229: gametophyte development
GO:0042180: cellular ketone metabolic process
GO:0010102: lateral root morphogenesis
GO:0006349: regulation of gene expression by genetic imprinting
GO:0006974: cellular response to DNA damage stimulus
GO:0050684: regulation of mRNA processing
GO:0040034: regulation of development, heterochronic
GO:0006625: protein targeting to peroxisome
GO:1903046: meiotic cell cycle process
GO:0043966: histone H3 acetylation
GO:0009110: vitamin biosynthetic process
GO:0006903: vesicle targeting
GO:0006955: immune response
GO:0009266: response to temperature stimulus
GO:0009756: carbohydrate mediated signaling
GO:0048359: mucilage metabolic process involved in seed coat development
GO:0016053: organic acid biosynthetic process
GO:0006367: transcription initiation from RNA polymerase II promoter
GO:0043632: modification-dependent macromolecule catabolic process
GO:0010051: xylem and phloem pattern formation
ath00600: Sphingolipid metabolism
GO:0009414: response to water deprivation
0
1
2
3
4
5
6
7
-log10(P)
(e)
GO:0010154: fruit development
GO:0010090: trichome morphogenesis
GO:0022402: cell cycle process
GO:0009888: tissue development
GO:0009909: regulation of flower development
GO:0042742: defense response to bacterium
GO:0033206: meiotic cytokinesis
GO:0051276: chromosome organization
GO:0060992: response to fungicide
GO:0032504: multicellular organism reproduction
GO:0048229: gametophyte development
GO:0033692: cellular polysaccharide biosynthetic process
GO:0010413: glucuronoxylan metabolic process
GO:0006349: regulation of gene expression by genetic imprinting
GO:0000710: meiotic mismatch repair
GO:0048284: organelle fusion
GO:0051130: positive regulation of cellular component organization
GO:0048585: negative regulation of response to stimulus
GO:0010051: xylem and phloem pattern formation
GO:0048878: chemical homeostasis
GO:0061647: histone H3-K9 modification
GO:0009867: jasmonic acid mediated signaling pathway
M00086: beta-Oxidation, acyl-CoA synthesis
GO:0071804: cellular potassium ion transport
GO:0010016: shoot system morphogenesis
GO:0006074: (1->3)-beta-D-glucan metabolic process
GO:0010216: maintenance of DNA methylation
GO:0034063: stress granule assembly
GO:0051186: cofactor metabolic process
GO:0071470: cellular response to osmotic stress
GO:0035690: cellular response to drug
GO:0046677: response to antibiotic
GO:0030163: protein catabolic process
GO:0051606: detection of stimulus
GO:0006352: DNA-templated transcription, initiation
GO:2000243: positive regulation of reproductive process
GO:0015766: disaccharide transport
GO:0010605: negative regulation of macromolecule metabolic process
GO:0051173: positive regulation of nitrogen compound metabolic process
GO:0031145: anaphase-promoting complex-dependent catabolic process
GO:0006766: vitamin metabolic process
GO:0009416: response to light stimulus
M00171: C4-dicarboxylic acid cycle, NAD - malic enzyme type
0
2
4
6
8
-log10(P)

Fig. 7

Gene expression variations in RNAi-*ddm1-23* vs the wild-type (WT) line (*Populus tremula* x *Populus alba*) under the water deficit/rewatering condition (WD-RW) in shoot apical meristems collected 1 wk after rewatering (t_2). (a) Geno ontology (GO) annotation of the differentially expressed genes (DEGs; genes with a false discovery rate (FDR)-adjusted *P*-value < 0.05; 136 DEGs identified) between RNAi-*ddm1-23* and the WT. Gene ontology labels were retrieved from PopGenIE and a heatmap was produced with METASCAPE. (b) Annotation of DEGs with expression variation values (log2FoldChange) using GO labels retrieved from PopGenIE. Blue dots denote downregulated genes and red triangles upregulated genes. Asterisks (*) indicate hormone related genes found among DEGs; dollar symbols ($) represent DEGs overlapping with DMRs; the hash symbol (#) represents DEGs that overlap with TEs; and the numbers (1), (31), (8), (25), (19), (17), and (35) represent the numbers of DEGs found corresponding to cell death, defense & cell wall, immune response, metabolism, signalization, transcription factors and unknown processes, respectively. Log2FoldChange = log-ratio of normalized mean read counts in RNAi-*ddm1-23* vs WT lines (*n* = 3 biological replicates for each line).

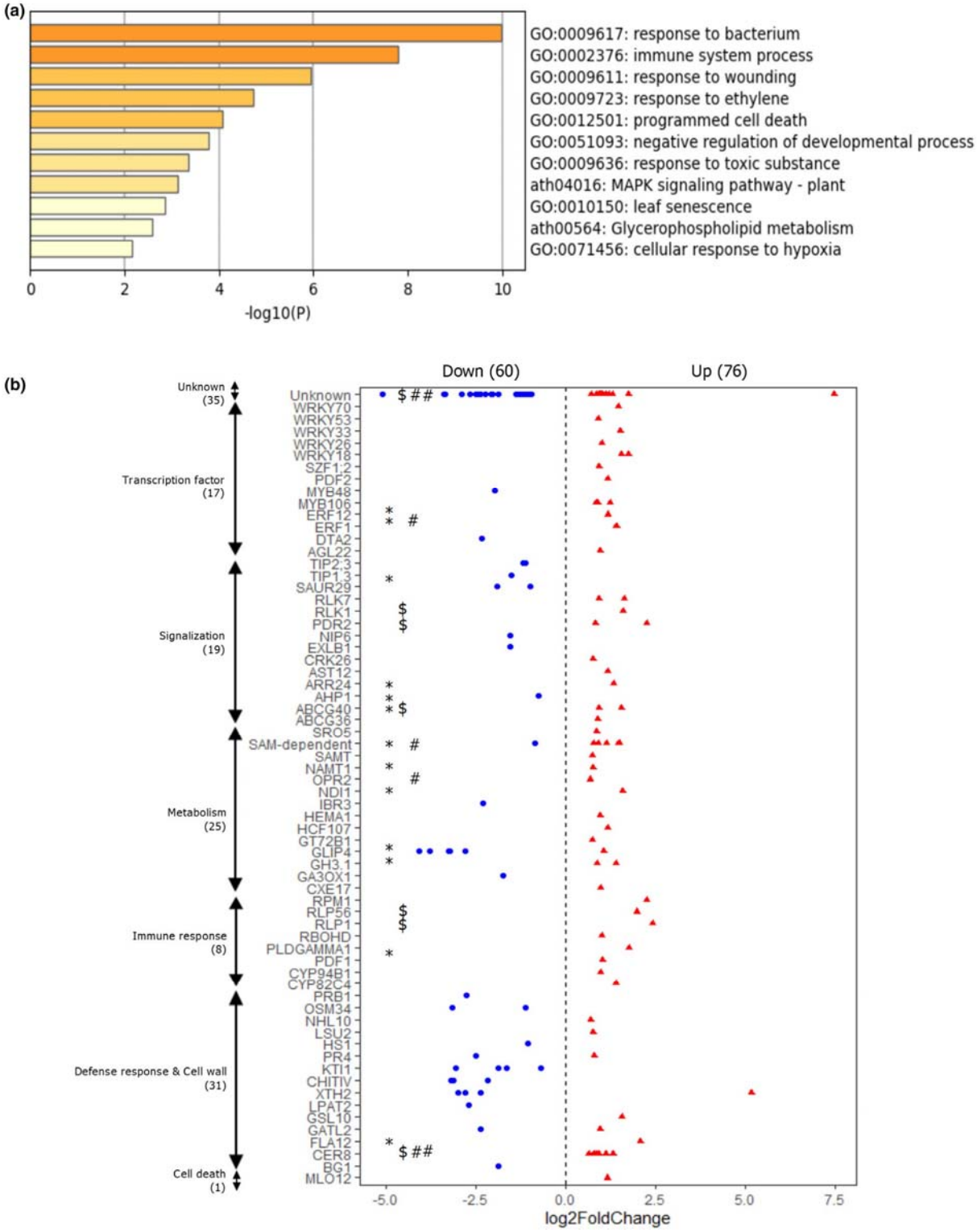
(a)
GO:0009617: response to bacterium
GO:0002376: immune system process
GO:0009611: response to wounding
GO:0009723: response to ethylene
GO:0012501: programmed cell death
GO:0051093: negative regulation of developmental process
GO:0009636: response to toxic substance
ath04016: MAPK signaling pathway - plant
GO:0010150: leaf senescence
ath00564: Glycerophospholipid metabolism
GO:0071456: cellular response to hypoxia
0
2
4
6
8
10
-log10(P)
(b)
Down (60)
Up (76)
Unknown (35)
Transcription factor (17)
Signalization (19)
Metabolism (25)
Immune response (8)
Defense response & Cell wall (31)
Cell death (1)
Unknown
WRKY70
WRKY53
WRKY33
WRKY26
WRKY18
SZF1.2
PDF2
MYB48
MYB106
ERF12
ERF1
DTA2
AGL22
TIP2.3
TIP1.3
SAUR29
RLK7
RLK1
PDR2
NIP6
EXLB1
CRK26
AST12
ARR24
AHP1
ABCG40
ABCG36
SRO5
SAM-dependent
SAMT
NAMT1
OPR2
NDI1
IBR3
HEMA1
HCF107
GT72B1
GLIP4
GH3.1
GA3OX1
CXE17
RPM1
RLP56
RLP1
RBOHD
PLDGAMMA1
PDF1
CYP94B1
CYP82C4
PRB1
OSM34
NHL10
LSU2
HS1
PR4
KTI1
CHITIV
XTH2
LPAT2
GSL10
GATL2
FLA12
CER8
BG1
MLO12
-5.0
-2.5
0.0
2.5
5.0
7.5
log2FoldChange

Fig. 8

Transposable element activity in RNAi-*ddm1* and wild-type (WT) lines (*Populus tremula* x *Populus alba*) in shoot apical meristems (SAMs) collected 1 wk after rewatering (t_2). (a) Mobilome-seq depth of coverage (read per million, rpm) of different transposable element (TE) families in wild-type (WT) and RNAi-*ddm1-23* lines and in both well-watered (WW, open diamonds, 115 and 44 families for WT and RNAi-*ddm1-23*, respectively) and water deficit followed by rewatering (WD-RW, closed triangles, 149 and 109 for WT and RNAi-*ddm1* -23, respectively) conditions. The coverage was calculated for each TE family and families are represented according to their superfamily. The four most active TE families are annotated: *Gyspy*23 (*G23*), *Gypsy*27 (*G27*), *DNA-3-3* (*D3*), *SAT-1* (*S1*). Transposable element activity was classified based on the sequencing coverage of eccDNA forms, as follows: TE (0 to 200 x); TE+ (200 x to 2000 x); TE++ (2000x to 10 000 x); TE+++ (10 000 x to 55 000 x). (b) DNA methylation variations at active TEs in RNAi-*ddm1* vs WT, represented for each context of methylation under WW (open plots) and WD-RW (closed plots) conditions. Note that no active TE could be detected inside a CHH differentially methylated region (DMR) under WW conditions. (c) DNA copy number variations analyzed by quantitative polymerase chain reaction (qPCR) on SAM genomic DNA for three different TE families (*DNA-3-3, Gypsy23* and *SAT-1*) in the WT and RNAi-*ddm1* -23 lines in both WW (open circles) and WD-RW (closed circles) conditions.

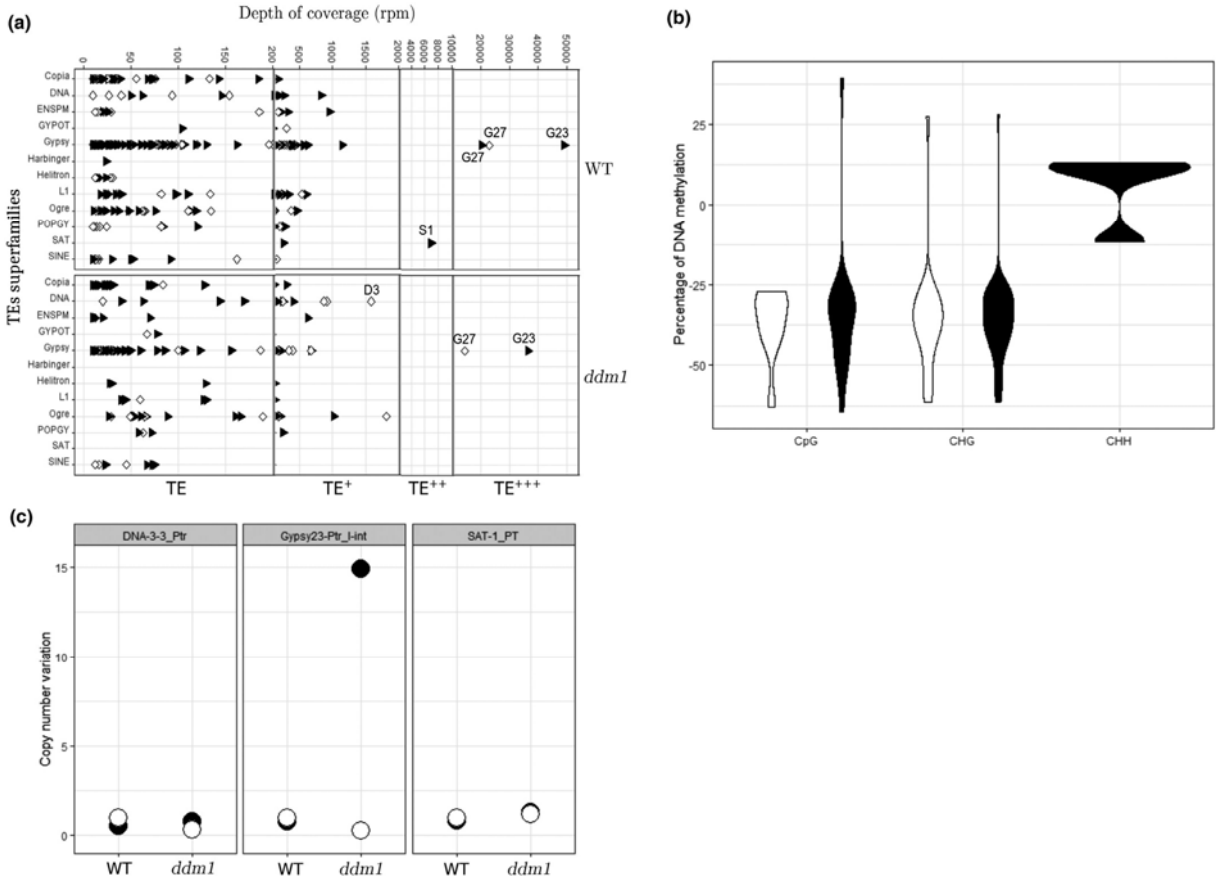

Table 1

Main characteristics of RNAi-*ddm1* vs wild type (WT) lines (*Populus tremula* x *Populus alba*).

Study scale and traits	Key results
Growth and drought tolerance	• RNAi-*ddm1* lines' height and diameter growth are not significantly affected by moderate water deficit • RNAi-*ddm1* lines are intrinsically more resistant to drought-induced cavitation
Leaf phenotypes	• RNAi-*ddm1* lines show necrotic spots independent of water availability
Phytohormones in the SAM	• RNAi-*ddm1* lines have higher SA concentrations in all tested conditions • RNAi-*ddm1* lines have lower zeatine riboside and lower zeatine-O-glucoside riboside (CKs) concentrations, but only under WD-RW
Methylome in the SAM	• RNAi-*ddm1* lines have hypomethylated SAMs • RNAi-*ddm1* lines show 5,374 (WW) / 5,172 (WD-RW) common DMRs compared to the WT; 1,736 were common to both conditions • RNAi-*ddm1* DMRs are context-dependent: CHG > CpG > CHH • RNAi-*ddm1* DMRs colocalize with 879 (WW) / 910 (WD-RW) genes (DMGs) and 23 (WW) / 89 TEs (WD-RW) • DMGs show GO enrichment in development, regulation of biological process and response to abiotic stress, including hormones
Transcriptome in the SAM	• 136 genes are differentially expressed in RNAi-*ddm1-23* vs WT in WD-RW conditions with GO enrichment in defense response, response to hormones and regulation of RNA metabolism • 53 differentially expressed genes correlate with the presence of RNAi-*ddm1* DMRs (at ± 10 kb) with a correlation between methylation and expression (Spearman's *rho* = −0.32 at $P = 0.0004$)
Mobilome in the SAM and qPCR	• 414 active TEs were detected in total (all lines and conditions), with 21% that colocalize with RNAi-*ddm1* DMRs • 92% of active TEs in DMRs are hypomethylated (CpG and CHG) in RNAi-*ddm1* lines but show CHH hypermethylation under WD-RW conditions • Two highly active TEs (*Gypsy* retrotransposons) show DNA copy number variation specifically in stressed (WD-RW) RNAi-*ddm1* lines

CK, cytokinin; DEG, differentially expressed gene; DMG, differentially methylated gene; DMR, differentially methylated region; GO, gene ontology; SA, salicylic acid; SAM, shoot apical meristem; TE, transposable element; WD-RW, water deficit-rewatering; WW, well-watered.